AD

CONTRACT REPORT ARBRL-CR-00514

PROJECTILE FOUNDATION MOMENT GENERATION

Prepared by

Battelle, Pacific Northwest Laboratory
P. O. Box 999
Richland, Washington 99352

June 1983

US ARMY ARMAMENT RESEARCH AND DEVELOPMENT COMMAND
BALLISTIC RESEARCH LABORATORY
ABERDEEN PROVING GROUND, MARYLAND

Destroy this report when it is no longer needed.
Do not return it to the originator.

Additional copies of this report may be obtained from the National Technical Information Service, U. S. Department of Commerce, Springfield, Virginia 22161.

The findings in this report are not to be construed as an official Department of the Army position, unless so designated by other authorized documents.

The use of trade names or manufacturers' names in this report does not constitute indorsement of any commercial product.

UNCLASSIFIED

SECURITY CLASSIFICATION OF THIS PAGE (When Data Entered)

REPORT DOCUMENTATION PAGE		READ INSTRUCTIONS BEFORE COMPLETING FORM
1. REPORT NUMBER CONTRACT REPORT ARBRL-CR-00514	2. GOVT ACCESSION NO.	3. RECIPIENT'S CATALOG NUMBER
4. TITLE (and Subtitle) PROJECTILE FOUNDATION MOMENT GENERATION		5. TYPE OF REPORT & PERIOD COVERED YEARLY REPORT FOR FY82 6. PERFORMING ORG. REPORT NUMBER
7. AUTHOR(s) E.M. PATTON F.A. SIMONEN L.A. STROPE		8. CONTRACT OR GRANT NUMBER(s)
9. PERFORMING ORGANIZATION NAME AND ADDRESS BATTELLE, PACIFIC NORTHWEST LABORATORY P. O. Box 999 Richland, Washington 99352		10. PROGRAM ELEMENT, PROJECT, TASK AREA & WORK UNIT NUMBERS 1L162618AH80
11. CONTROLLING OFFICE NAME AND ADDRESS US Army Armament Research & Development Command US Army Ballistic Research Laboratory (DRDAR-BLA-S) Aberdeen Proving Ground, MD 21005		12. REPORT DATE June 1983 13. NUMBER OF PAGES 65
14. MONITORING AGENCY NAME & ADDRESS(if different from Controlling Office)		15. SECURITY CLASS. (of this report) UNCLASSIFIED 15a. DECLASSIFICATION/DOWNGRADING SCHEDULE

16. DISTRIBUTION STATEMENT (of this Report)

Approved for public release; distribution unlimited.

17. DISTRIBUTION STATEMENT (of the abstract entered in Block 20, if different from Report)

18. SUPPLEMENTARY NOTES

19. KEY WORDS (Continue on reverse side if necessary and identify by block number)

Projectile Off-Axis Motion	Rotating Band
Balloting	Obturator
Yaw-In-Bore	In-Bore Dynamics
Rotating Band Moment	Gun Dynamics

20. ABSTRACT (Continue on reverse side if necessary and identify by block number) jmk

A project was initiated to develop methods to evaluate the magnitude of restoring foundation moment generated by cocking of an obturated projectile while in bore. An analytical and experimental study was undertaken to assess the magnitude of this foundation moment for a stationary projectile. The analytical portion of the study consisted of a finite element analysis conducted using the computer code ANSYS. An experimental apparatus was constructed to test the validity of the finite element approach.

(continued on next page)

DD FORM 1 JAN 73 1473 EDITION OF 1 NOV 65 IS OBSOLETE

UNCLASSIFIED

SECURITY CLASSIFICATION OF THIS PAGE (When Data Entered)

20. (continued)

The results of this study indicate that the foundation moment is large. A comparison of this foundation moment to the moment caused by an off-axis rotation of the center of gravity (yaw-in-bore) shows that the foundation moment is equivalent to having the center of gravity at least 2.68 in. (6.8 cm) behind the axial center of the obturator band of a 120-mm kinetic energy projectile.

TABLE OF CONTENTS

LIST OF ILLUSTRATIONS

LIST OF TABLES

INTRODUCTION

This study was conducted by Battelle's Pacific Northwest Laboratory (PNL) for the U.S. Army's Ballistic Research Laboratory (BRL). The purpose of this study was to develop methods to evaluate the magnitude of the restoring or foundation moment generated by cocking of an obturated projectile while it is within the bore of a gun. Saboted projectiles (KE-type) most commonly ride the bore of the gun during launch on what is called the obturator or drive band. Stability of the projectile in-bore is most often provided by two bore contact surfaces located at some distance from one another (i.e., a long "wheel base"). The rearward surface is provided by the plastic obturator, and the forward surface is either a plastic band or steel bourrelet which rides the gun bore. The use of two bore riding surfaces results in a greater parasitic weight of the projectile (the sabot) than if there were only one bore riding surface. A cross-section view of a typical KE projectile with a long "wheel base" is shown in Figure 1.

The purpose of this project is to develop analysis methods to be applied in the design of projectiles with one bore-riding surface and with good in-bore stability. One of the contributing factors to stability is the righting moment which occurs when the projectile begins to cock in bore. This righting moment will be a function of the stiffness of the plastic obturator or drive band and its resistance to local radial deformations. The characteristics of this band as well as the stiffness of the sabot are therefore very important in determining the resistance of the single bore contact projectile to balloting or wobbling in the bore of the gun.

In the case of the projectile with a long "wheel base," this wobbling resistance (termed foundation moment) is provided by the separation of two

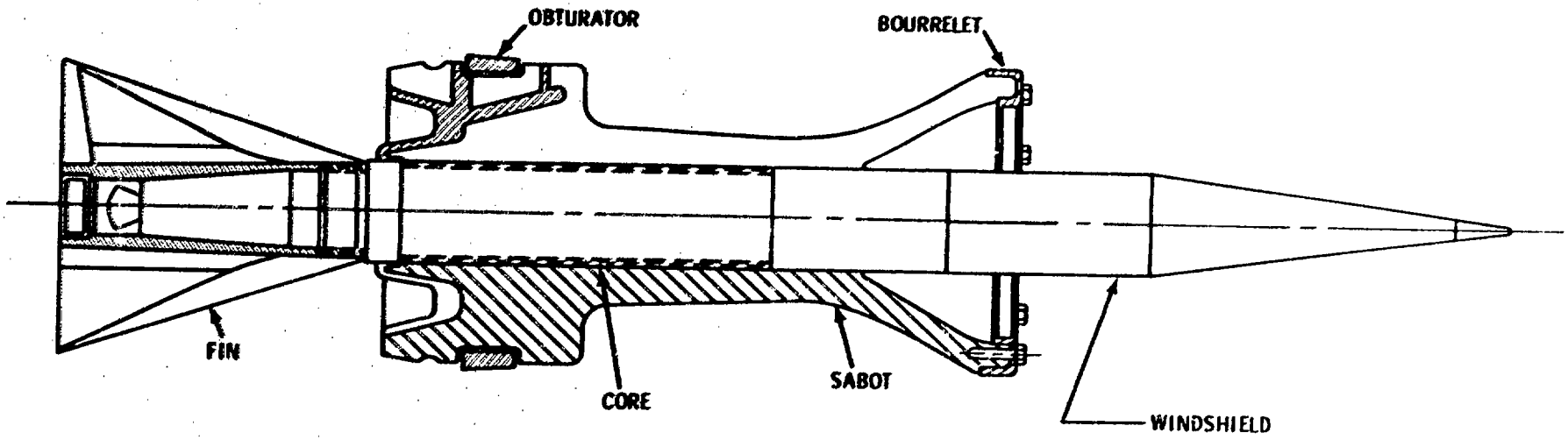

FIGURE 1. Cross Section Drawing of M735 - Similar in Design to Several Long "Wheel Base" KE Projectiles

line contacts with a fairly rigid member between them. In the case of the single bore contact projectile, this resistance to wobbling or foundation moment is provided by the stiffness of the obturator drive band.

This report describes an experimental and analytical study performed at PNL to estimate the foundation moment. A simplified but characteristic geometry was chosen which was simple both to model analytically and to fabricate for experimental studies. Three different finite element models were constructed for the purpose of evaluating alternate simulation techniques. An experimental apparatus was also constructed with the same geometry in order to verify the analytical models. This report documents the analysis, testing, and conclusions of the project thus far. For the sake of simplicity, this report looks at the problem in a nondimensional manner. The only time that actual dimensions are reported is in the Implications of Results section in which results of the analysis are scaled up to what would be seen in an actual gun tube.

FINITE ELEMENT MODELS

Following a meeting between BRL and PNL personnel in early January 1982, a geometry was chosen for the finite element and testing phase of the program. That geometry is shown in cross-section view in Figure 2. This figure shows a plot of a finite element mesh developed for the finite element code ANSYS.* All finite element stress analyses were performed with ANSYS. The large diameter portion of the model in Figure 2 is the "bore-riding" portion of the configuration, and the small diameter extension serves as the arm by which a moment can be applied to the "bore-riding" portion. The shaded area of the "bore-riding" part models the plastic band or obturator. This plastic band was restrained at its outer diameter in the radial direction. A transverse deflection was applied at the end of the arm, to apply a moment to the model. The finite element analysis calculated the reaction force at the deflected end of the arm which in effect gives the moment required to produce the known (prescribed) angular deflection.

ELEMENT AND MESH REFINEMENT STUDIES

Two-dimensional (2-D) axisymmetric finite element codes do not generally allow nonaxisymmetric loading such as that required for the present analysis. ANSYS, however, permits the nonaxisymmetric loading to be applied in the form of a sinusoidal variation around the circumference of the model. The variation is in the form of A sin Nθ, where A is the amplitude of the loading and N is the number of sine waves applied around the circumference. (One can also specify that the loading is A cos Nθ.) By adding up the results of several analyses the solution for a Fourier series type of loading can be obtained. For this work, only a single term is required to describe the 0.1-inch deflection at the end of the model (i.e., 0.1 cos θ).

** ANSYS is a proprietary engineering analysis computer program owned, marketed, and supported by Swanson Analysis Systems, Inc.*

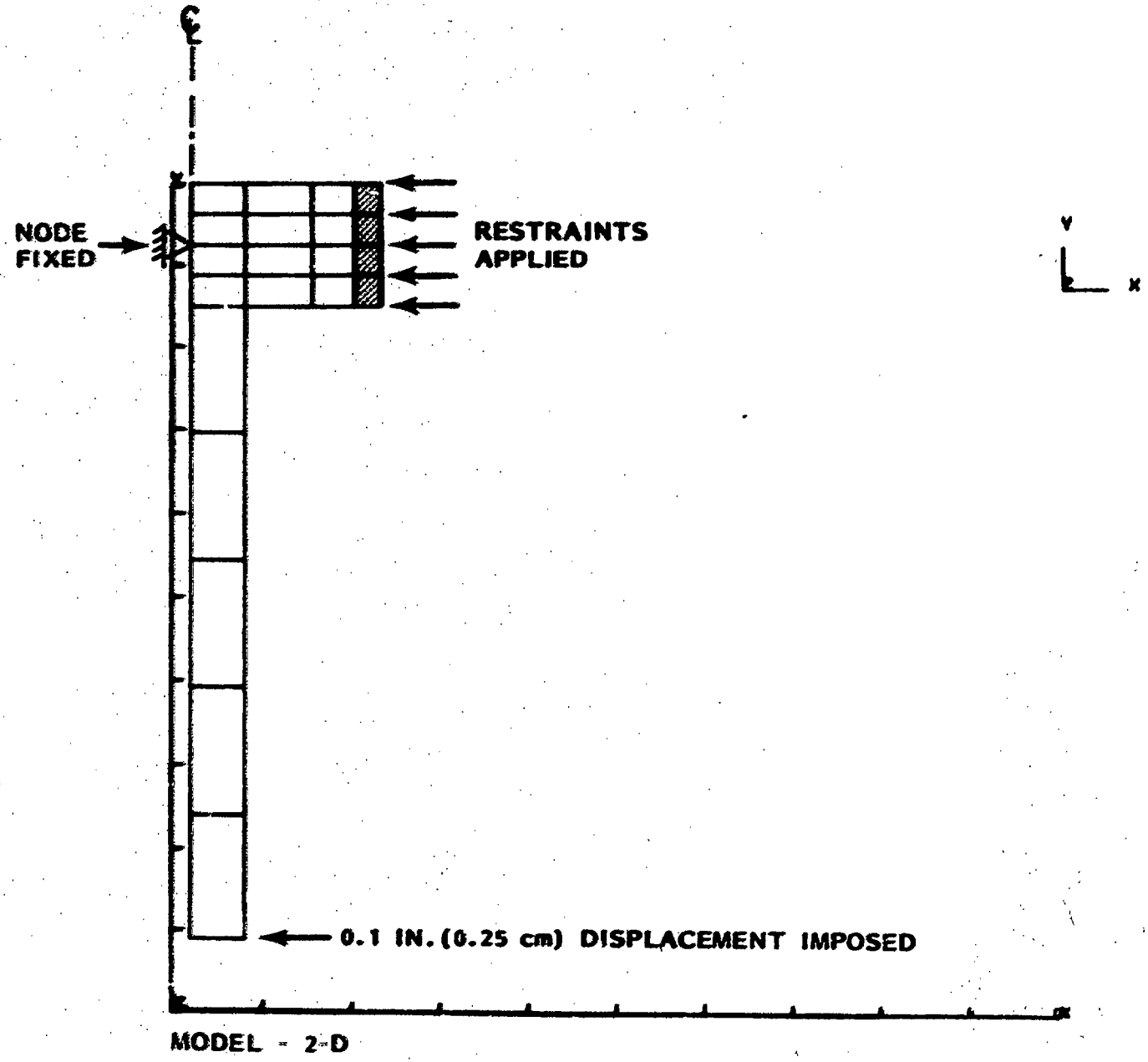

FIGURE 2. Cross Section of Analyzer and Tested Geometry

It is possible that the 2-D representation with nonaxisymmetric loading can give more accurate results than a model using 3-D finite elements. The 3-D model, for the same cost per computation, must be meshed coarsely in the circumferential direction. This will cause numerical errors not present in the 2-D axisymmetric model, which treats circumferential variations in stress in an "exact" analytical manner. The 2-D element used in ANSYS does not, however, allow material nonlinearities in conjunction with nonaxisymmetric loadings. It is expected that the plastics used for obturator materials will not behave in a linear elastic fashion at the stress levels imposed during launch of a projectile. The ANSYS 3-D element can treat material nonlinearity, and for this reason, a 3-D model was also developed as shown in Figure 3. The 2-D model was used primarily as a guide for evaluating the circumferential mesh refinement for the 3-D models.

A three-dimensional finite element analysis can involve considerable computing costs, since the number of nodes and elements increase rapidly with the level of refinement of the mesh. In this case, the refinement of concern is in the circumferential direction. The cost of a finite element analysis goes up at least in proportion to the increase in number of nodes and elements, since the number of degrees of freedom directly determines the size of the system of equations which has to be solved. Nonlinear materials require iterative solutions, which typically increase cost about an order of magnitude. For these reasons, it was desirable to determine an optimum circumferential mesh refinement for the 3-D analysis.

The 3-D model as shown in Figure 3 has a moment applying arm, a bore-riding portion and a plastic band (i.e., shaded region). This model is meshed into 30 degree segments circumferentially. The element used is the 3-D extension of the 2-D isoparametric quadrilateral used in the axisymmetric model. It is often described as an 8-node brick element. The fact that element stresses are computed by ANSYS only at the element

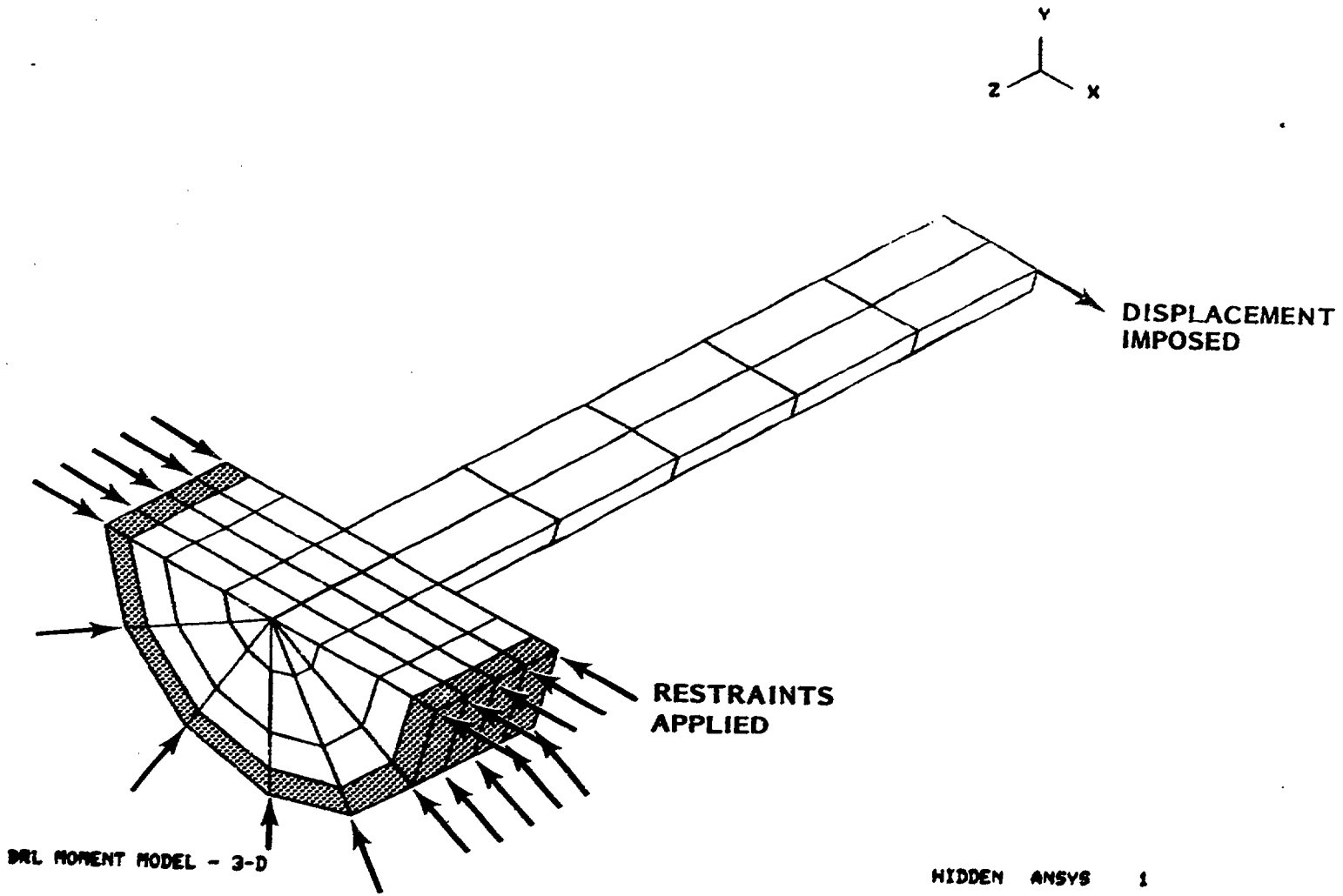

FIGURE 3. 3-D Finite Element Model Mesh Showing Restraints, Imposed Displacement, and Imposition of the Symmetry Condition

centroid gives rise to less detailed stress output than the 2-D models. The 3-D element does, however, allow material nonlinearities in the form of inelastic strains which will occur in the obturator material during launch of a projectile.

Another finite element model was developed as a further check on the 2-D axisymmetric model with nonaxisymmetric loading. This model treats the large bore-riding part of the chosen geometry as seen in an end on view. This model, shown in Figure 4, is essertially a flat circular plate of unit (1 in.) (2.54 cm) thickness. It is constrained radially (radial displacement = 0) at its outside edge and a small radial displacement (0.01 in.) (0.0254 cm) is imposed at its center. The circumferential mesh increment is 5 degrees. The 2-D axisymmetric and 3-D models were also constrained and loaded in this fashion. In addition, the 3-D model mesh was refined circumferentially from 30 degrees per element to 15 degrees and 10 degrees. In this manner, a sensitivity study was performed to study the effects of mesh refinement of the 3-D models. The results are shown in Figure 5. Note that all of the models produced results that differed by less than 10 percent and that even the 3-D model with 30 degree elements produced good results. It was thought, however, that a 15 degree circumferential mesh refinement, although not required in the linear elastic analyses, would be desirable when material nonlinearities were added to the model. The 15 degree circumferential mesh refinement was therefore chosen for the remainder of the 3-D modelling.

FURTHER ANALYSIS

The material properties used initially for the plastic band were taken from handbook values. It was also originally thought that a rigid representation of the metal parts would be adequate. For the plastic band material values of 175,000 psi (1207 MPa) for Young's modulus and 0.4 for

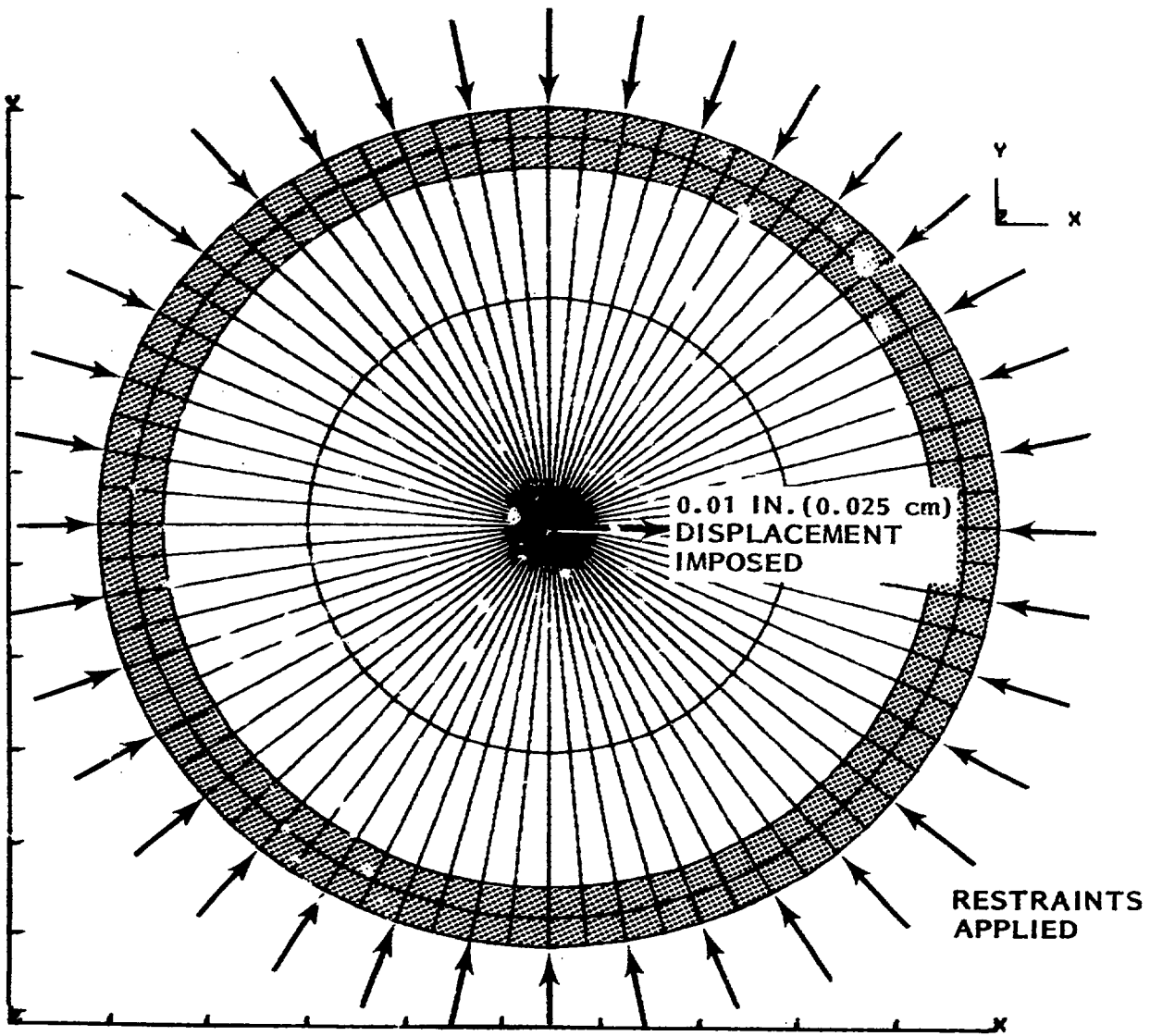

FIGURE 4. 2-D End-On Model of Test Fixture Showing 5 Degree Circumferential Mesh Size, Plastic Band, Restraints, and Imposed Displacement

Poisson's Ratio were chosen on the basis of manufacturers' data[1] and discussions with staff in PNL's Materials Department. These values and a Young's modulus of 30 X 10^8 psi (20.7 x 10^6 MPa) (2 orders of magnitude more stiff than steel) for the metal core of the model produced the results shown in Figure 5.

During the course of this project several aspects of the models used in the above described element selection and mesh refinement study were changed. The most notable changes were the properties of the plastic used for obturator band material, and the geometry of the metal portion of the model. A small variation in the banded (bore-riding) part of the model was required to produce a band that would not slip during testing. That geometry is shown in Figure 6. It is essentially identical to that shown in Figure 3 except that the plastic band has a thicker portion which fits into a central depression in the metal core. This eliminated any possibility of slip in the axial direction at the core-plastic interface.

A second, much more significant change had to be made in the geometry of the moment-applying bar portion of the model. Initial testing and analysis showed an unexpectedly high moment generated by the plastic band and associated bending of the bar. Therefore, it was decided to stiffen the bar considerably.

The elastic properties of the plastic obturator material were also changed during the course of this project. Initial handbook values for Young's modulus proved to be much lower than the actual material used in the testing phase of this work. Material tests performed as part of this project are described in another section of this report.

---

[1] *DuPont Plastics Design Handbook, page 15, Table 5.*

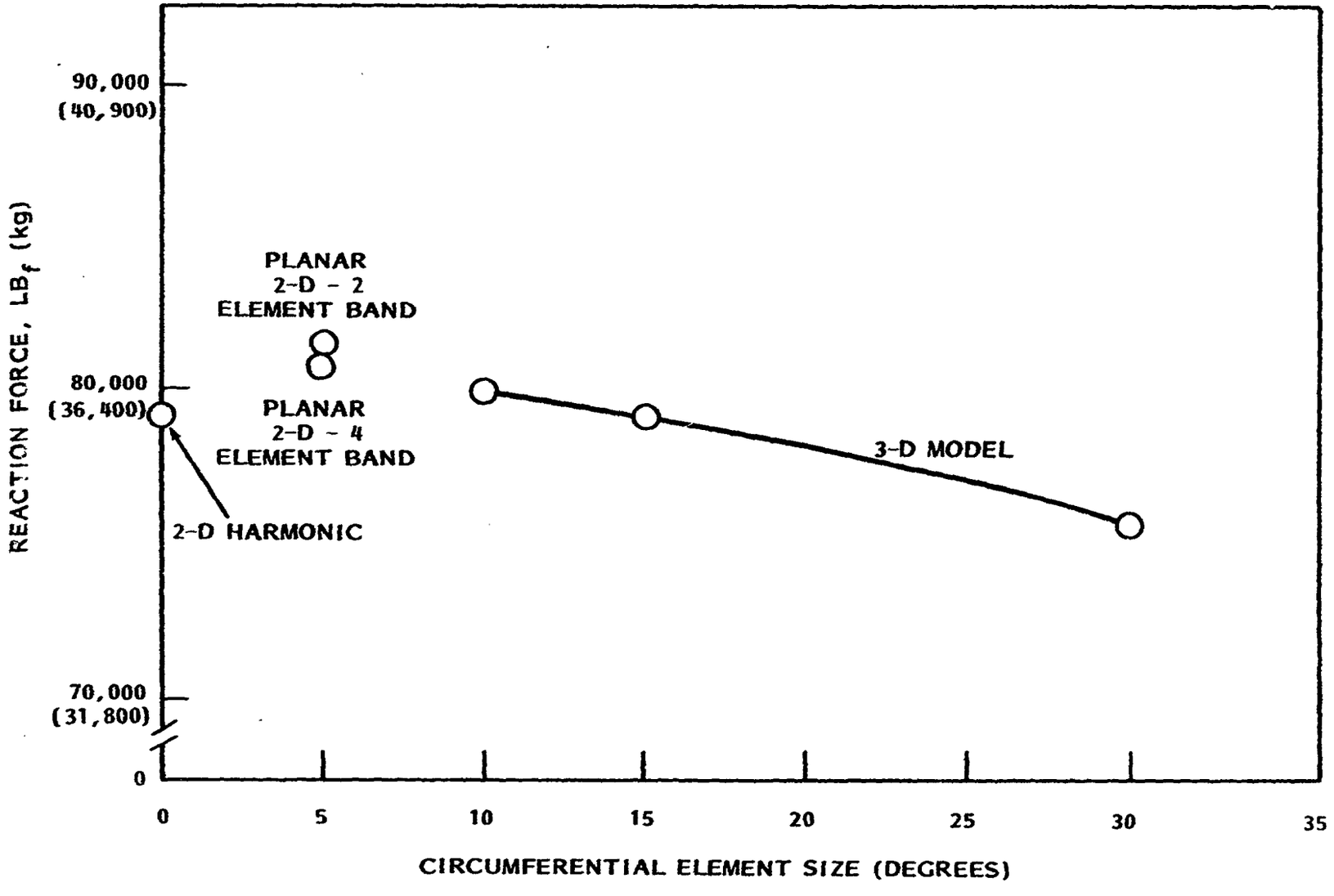

FIGURE 5. Results of Circumferential Mesh Size Sensitivity Study

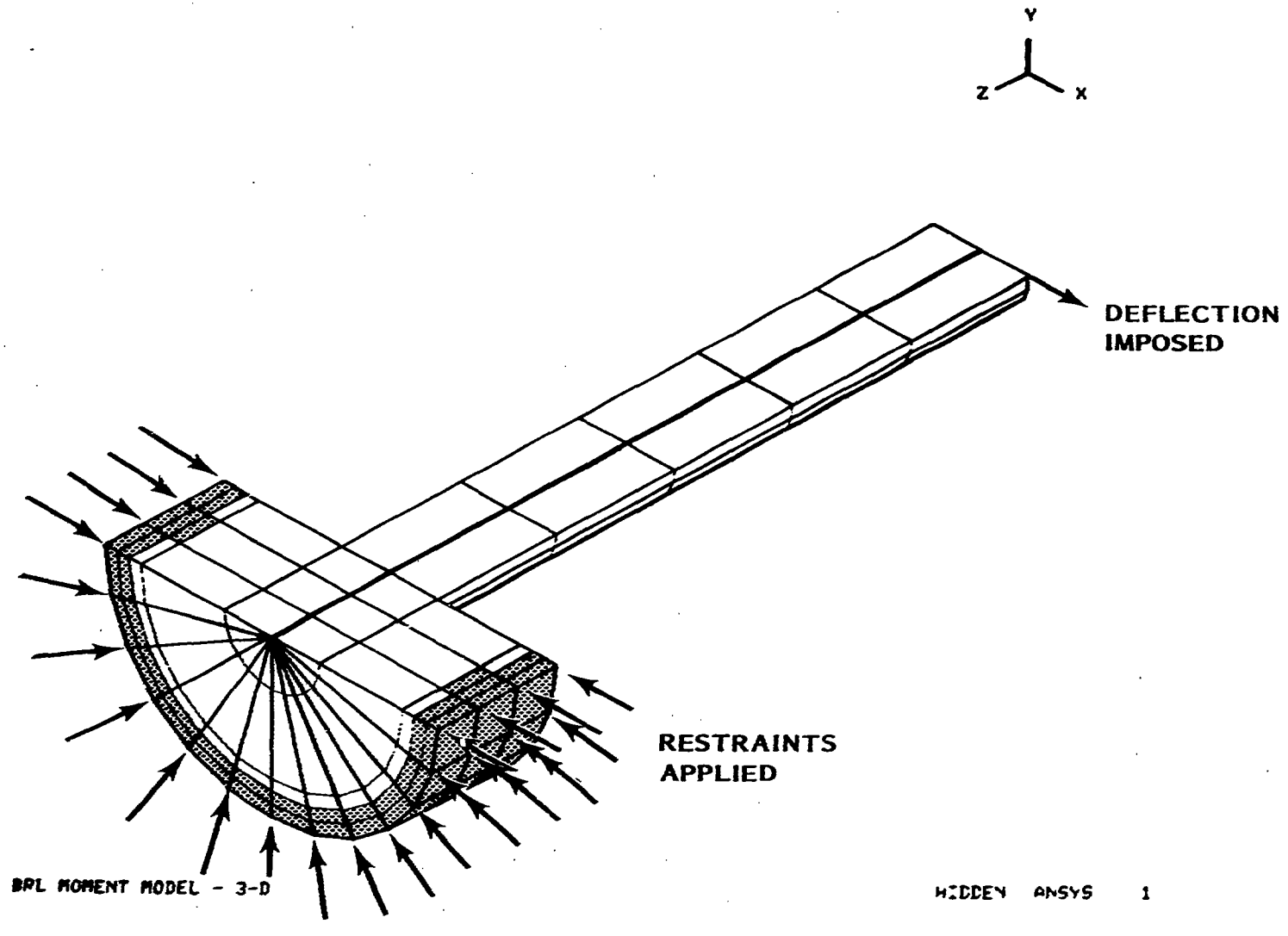

FIGURE 6. Revised Version of 3-D Model With Slotted Band and 15 Degree Circumferential Element Size

TEST FIXTURE

The original test fixture built to measure the foundation moment is shown in Figure 7. Figure 8 shows a series of photographs of the fixture in the load frame used for the tests. Figure 9 is a schematic of the original test fixture. The central portion of the assembly is made of aluminum bar stock. The aluminum portion comes apart in the middle to allow installation of the plastic band. Four hardened cap screws were used to fasten the aluminum end cap which holds the plastic band in place. Once this aluminum and plastic assembly is put together, it is bolted into the steel frame shown schematically in Figure 9 and pictorially in Figures 7 and 8. This steel frame consists of a bottom plate and an upright member which is split horizontally to allow installation of the aluminum and plastic assembly. In this fashion, a simulated projectile (aluminum and plastic assembly) is assembled into a short section of a simulated gun tube (steel clamping device). The inside of the steel clamping fixture and the outer surface of the plastic band had machined grooves to prevent slippage along the plastic-steel interface. To ensure proper clamping of the aluminum and plastic assembly, an interference of approximately 0.005 in. (0.013 cm) was provided in the steel clamping device. The bottom of the upper semicircular clamp was machined off to provide this interference.

The plastic band in the test fixture was machined from a tube of nylon ordered from DuPont. The tube is centrifugally cast ZYTEL 101 with an outside diameter of 3-1/8 in. (7.9 cm) and an inside diameter of 1-1/4 in. (3.2 cm). The material was specified with a military specification common to most of the KE obturators. This specification is: nylon tube, centrifugally cast, ZYTEL 101, composition "A," Type I, MIL-M-20693.

This entire assembly was placed in a load frame. This frame consisted of a handcranked bottom platen which moves the specimen up to contact a

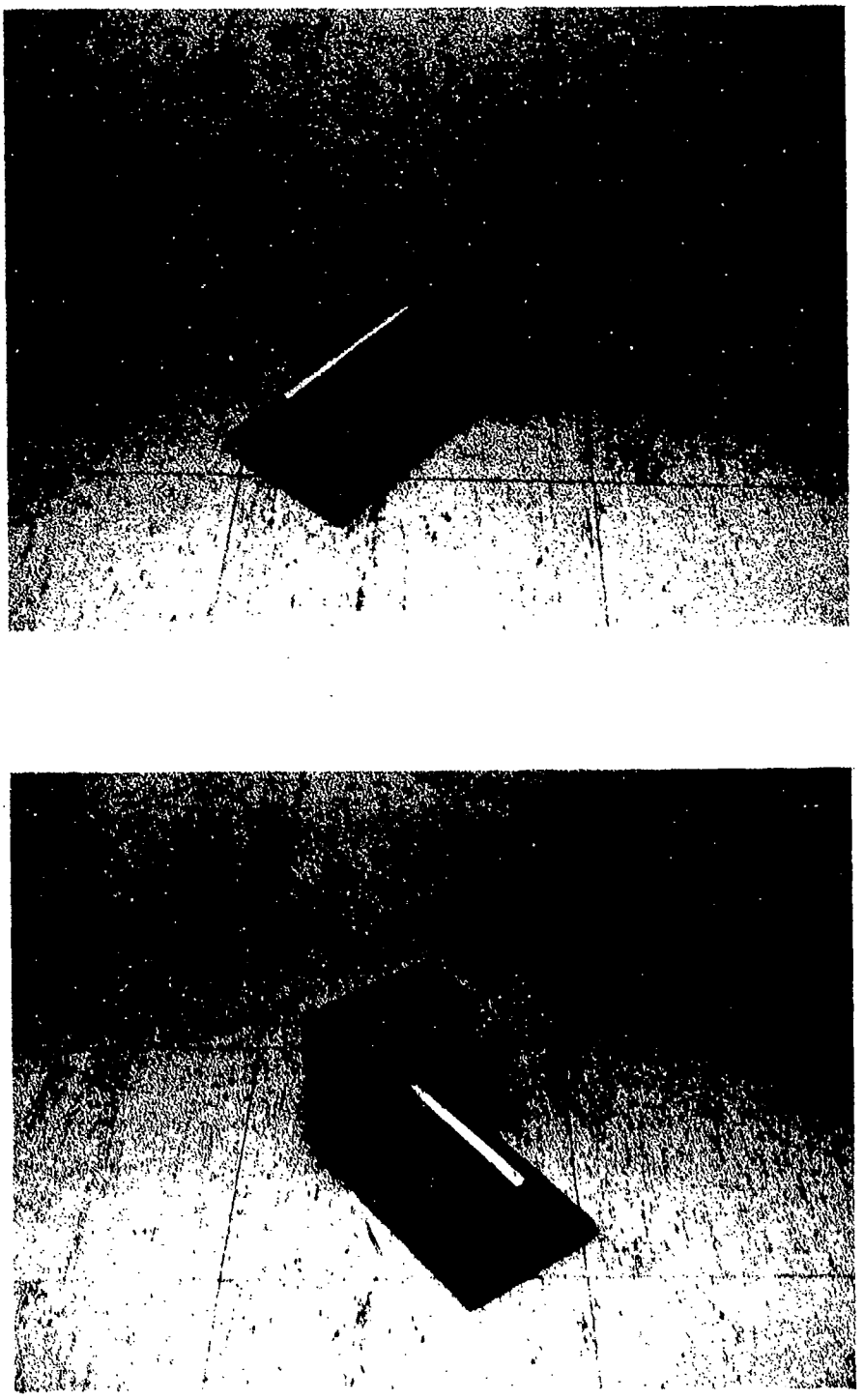

FIGURE 7. Photographs of Original Test Fixture

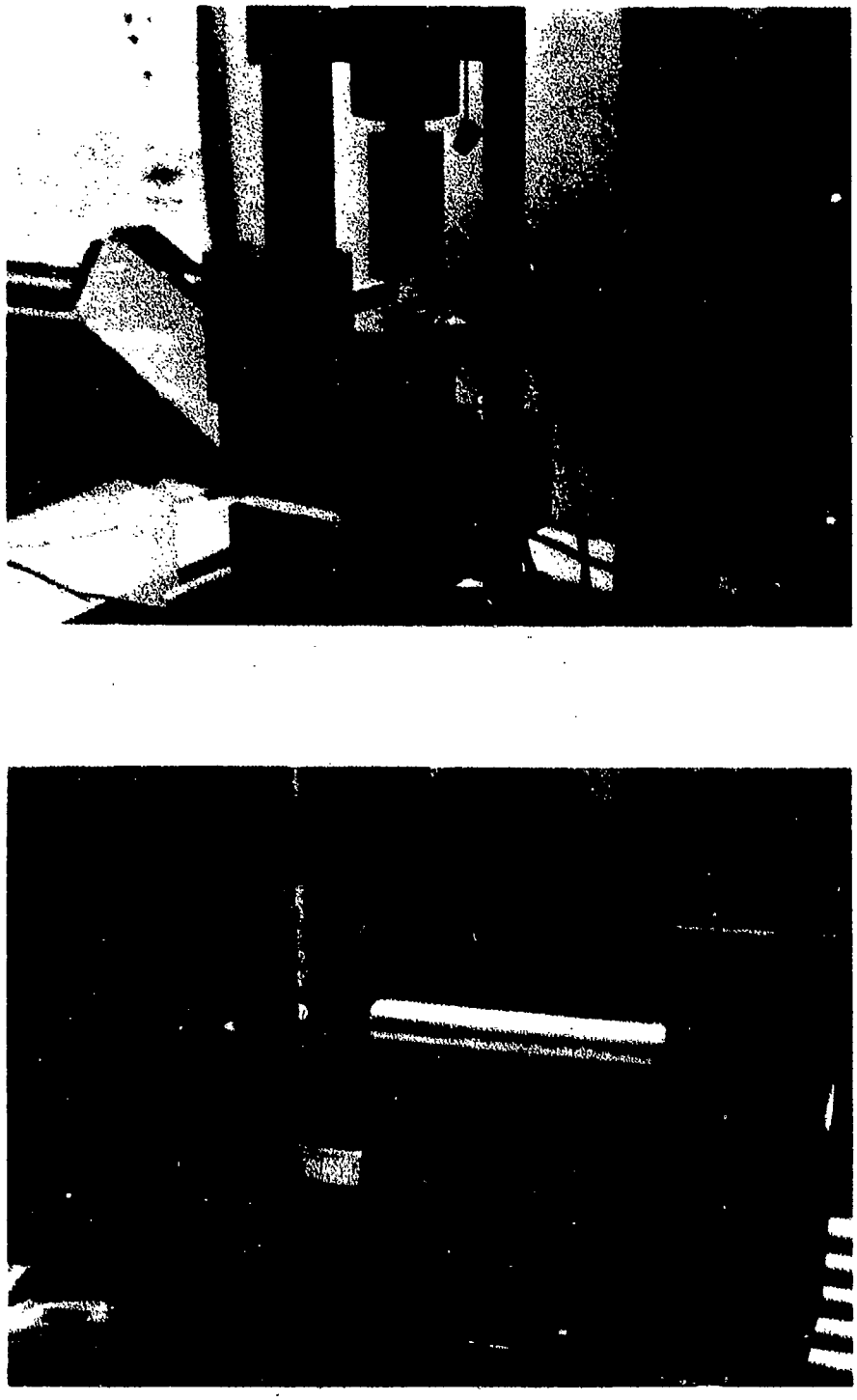

FIGURE 8. Photographs of Test Fixture Installed in its Load Frame. Note Load Cell and Clip Gage

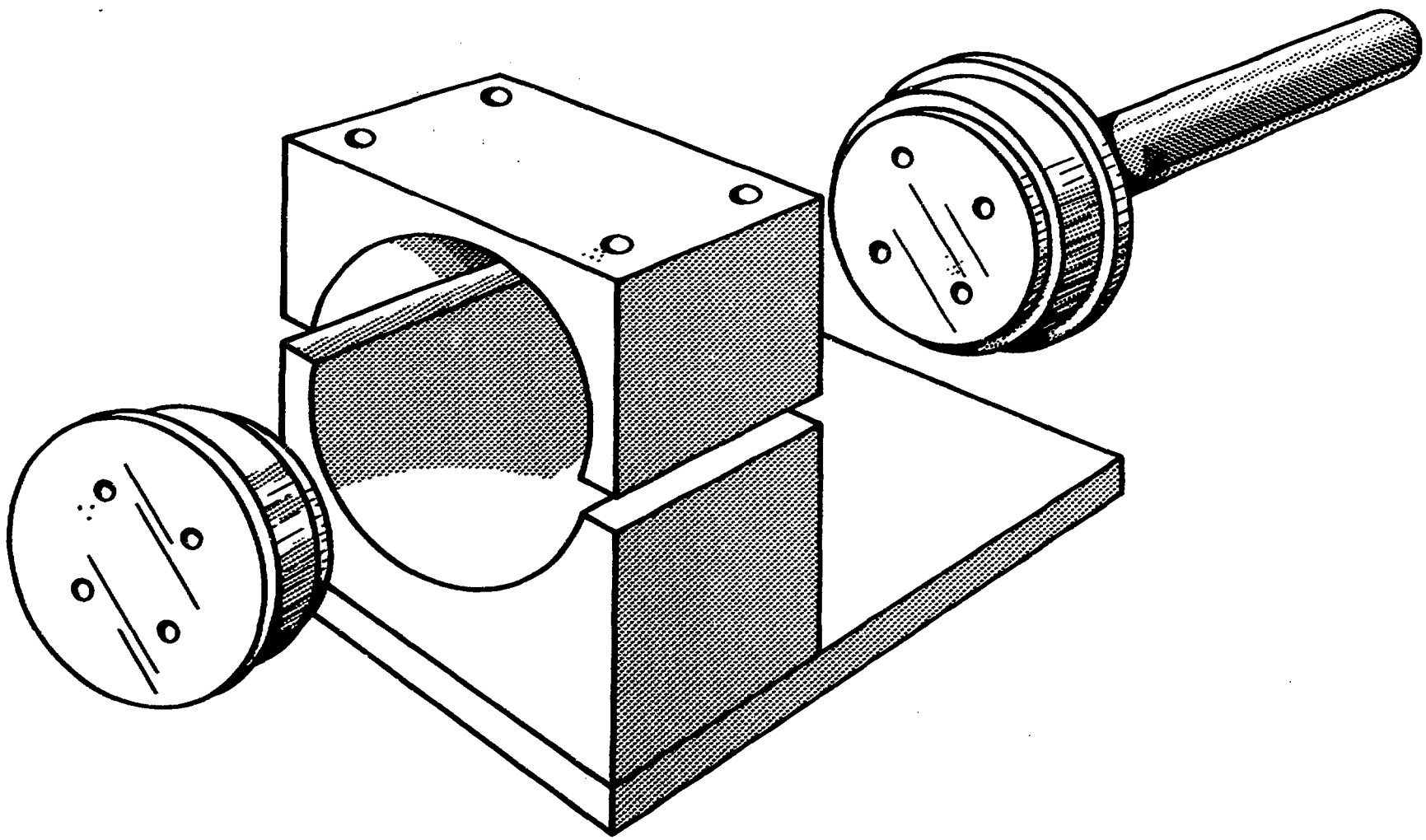

FIGURE 9. Schematic of Original Test Fixture

mandrel which is bolted to a BLH Electronics Type UG32 load cell. The load cell signal was conditioned with a Doric Digital Transducer Indicator Model 420 with analog output. The capacity of this load frame was 10,000 lbf (5450 kg). A clip gauge was placed between the bottom plate of the fixture and the end of the moment applying arm (aluminum arm). This clip gauge is a doubly cantilevered gauge with four micromeasurement strain gauges connected in a wheatstone bridge. The output signal from the gauge was conditioned with an Endevco Model 4470 voltage regulator bridge conditioner. This signal, combined with the output from the BLH electronics load cell, was fed to a Honeywell Model 1540 X-Y chart recorder. The entire system was calibrated and used to obtain a plot of force versus deflection at the end of the aluminum bar.

TEST RESULTS VS. FINITE ELEMENT ANALYSIS

The results of the first test are shown in Figure 10. Note that the force required to deflect the end of the aluminum bar by 0.1 in. (0.25 cm) was about 180-190 lbf (82-86 kg). The initial finite element analyses treated the metallic parts as essentially rigid because it was thought that the resisting moment (foundation moment) would be fairly small. It is most commonly treated as a higher order effect in ballistic analyses of projectiles.

The initial analyses predicted forces much greater than the 190 lbf (86 kg) output from the test. The forces calculated by ANSYS were in excess of 1300 lbf (590 kg) and in one case as high as 8200 lbf (3720 kg), computed by using different restraint conditions. Explanations were sought for the obvious difference between the analysis and the test. A possible source of the discrepancy was the compliance of the test fixture. To check for compliance the actual modulus of elasticity (10×10^6 psi) (69×10^3 MPa) was used for the aluminum central portion in the ANSYS model. The calculated reaction force at the end of the aluminum bar dropped from 1390 lbf (630 kg) to 325 lbf (147 kg). The fixture was obviously much too compliant to be modeled as a rigid member in the finite element simulation. Figure 11 portrays graphically the difference between a rigid center and an aluminum center. It is a plot of the centerline deflection (as calculated by ANSYS) of the fixture for two cases; one with the center portion modelled as rigid ($E = 30 \times 10^8$ psi) (20.7×10^6 MPa), and one for an aluminum center ($E = 10 \times 10^6$ psi) (69×10^3 MPa). Note that almost all of the deflection in the case of the aluminum center consists of bending in the bar.

To minimize undesired bending of the bar, a new central core was designed and manufactured from a single bar of 304 stainless steel. A

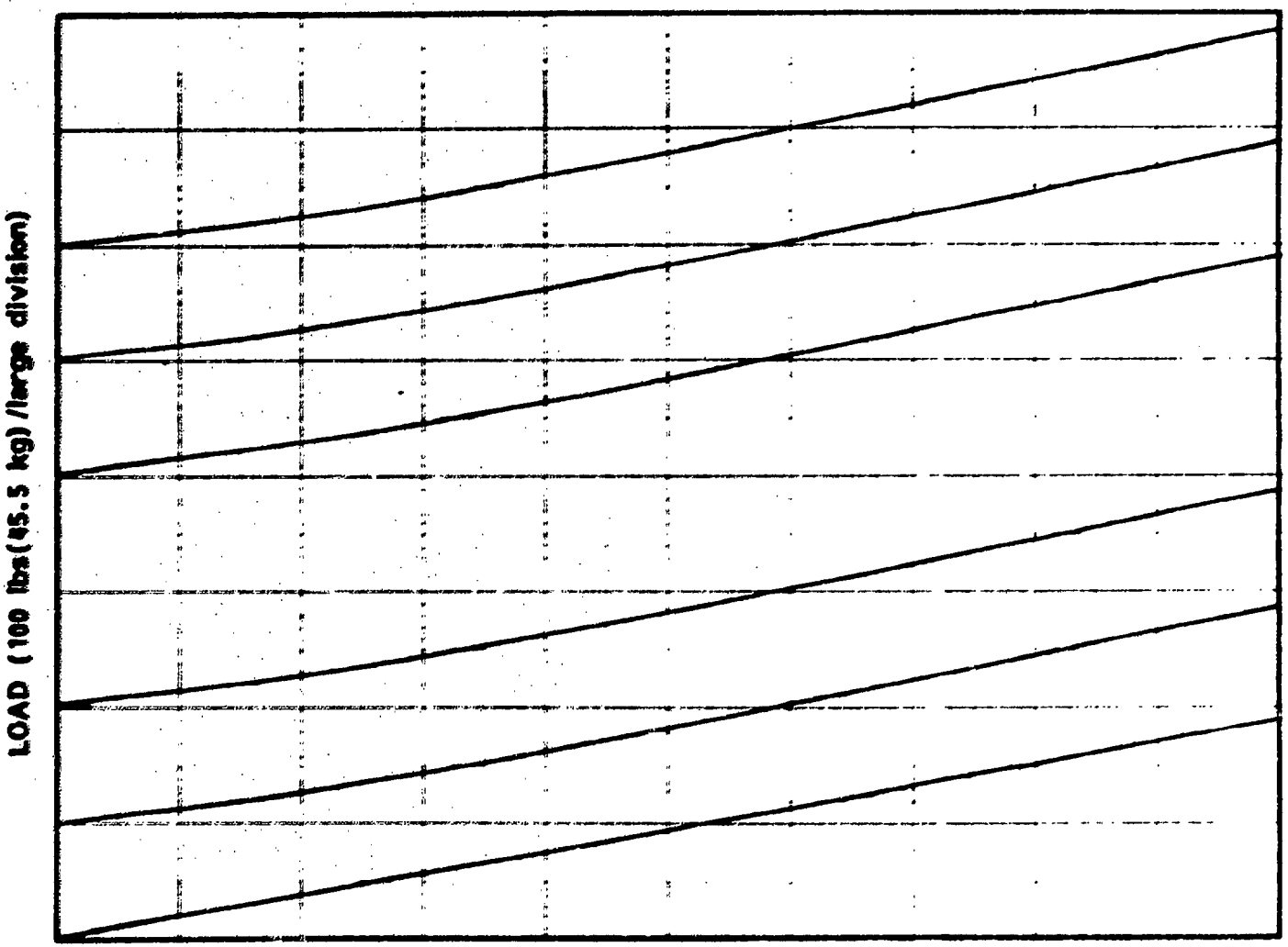

FIGURE 10. First Test Results

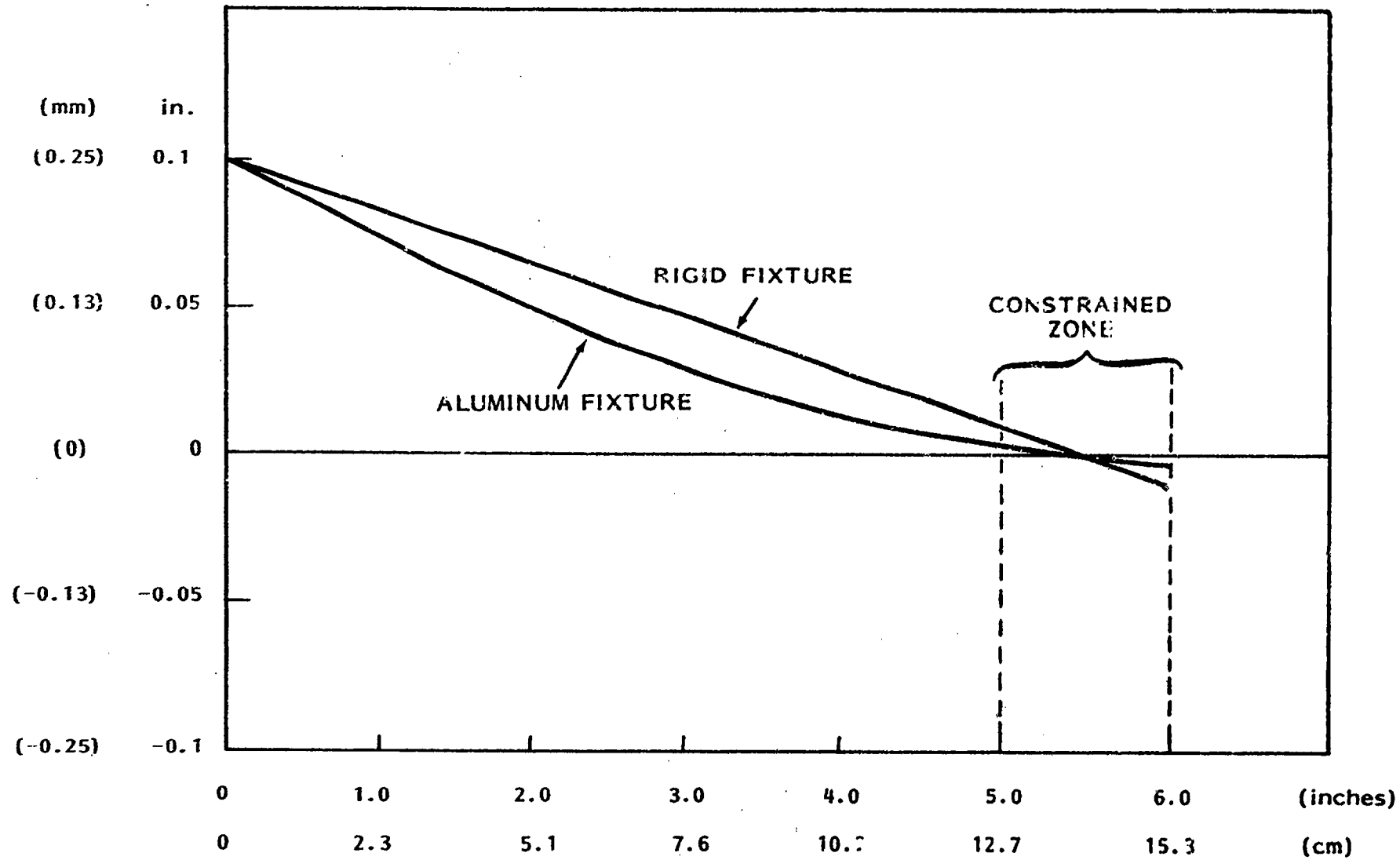

FIGURE 11. Centerline Deflection for Rigid Fixture and Aluminum Fixture

schematic of this central piece is shown in Figure 12, and photographs of it are shown in Figure 13. A slot was added to the rear portion of the arm to get clearance for the clip gauge in the test setup. The ANSYS model for this new central portion is shown in Figure 14. Because the interest was in the behavior at the plastic-to-bore interface, it was unnecessary to add the notch geometry to the ANSYS model. The results for this ANSYS model which treated the compliance of the stainless steel rod (1314 lbf) (597 kg) were reasonably close to the results of the rigid center case (1375 lbf) (624 kg).

The tested results for this new central core clamped in the original fixture are shown in Figure 15. The clamping fixture was then also stiffened as shown in the photographs of Figure 16. The results of tests with the newly revised fixture are shown in Figure 17. If the measurements from the last test are corrected for bolt stretch in the clamping device and for bending of the bottom plate of the clamping device, the test data indicate that it will require approximately 1800 lbf (810 kg) to deflect the end of the fixture 0.02 in. (.05 cm). Further predictions were made using ANSYS. These predictions use a 0.02 in. (0.05 cm) fixture end deflection, the stainless steel core, and a nylon elastic modulus of 600,000 psi (4140 MPa). The measured result of 1800 lbf (810 kg) is bounded by two predictions varying boundary conditions: fixed axially and radially at the plastic gun bore interface, and fixed radially only at this interface.

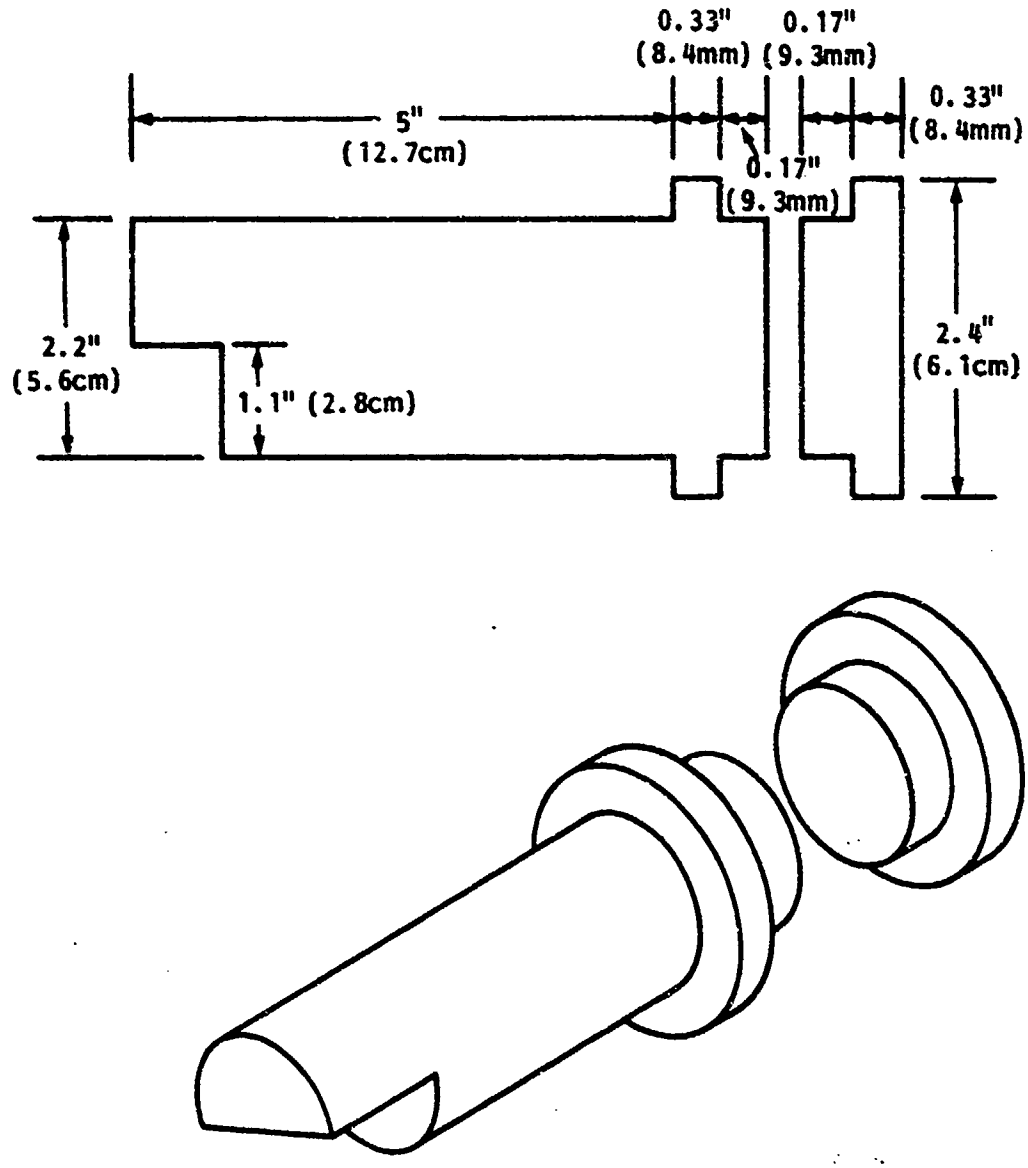

FIGURE 12. New Fixture Central Core, Machined From Type 304 Stainless Steel

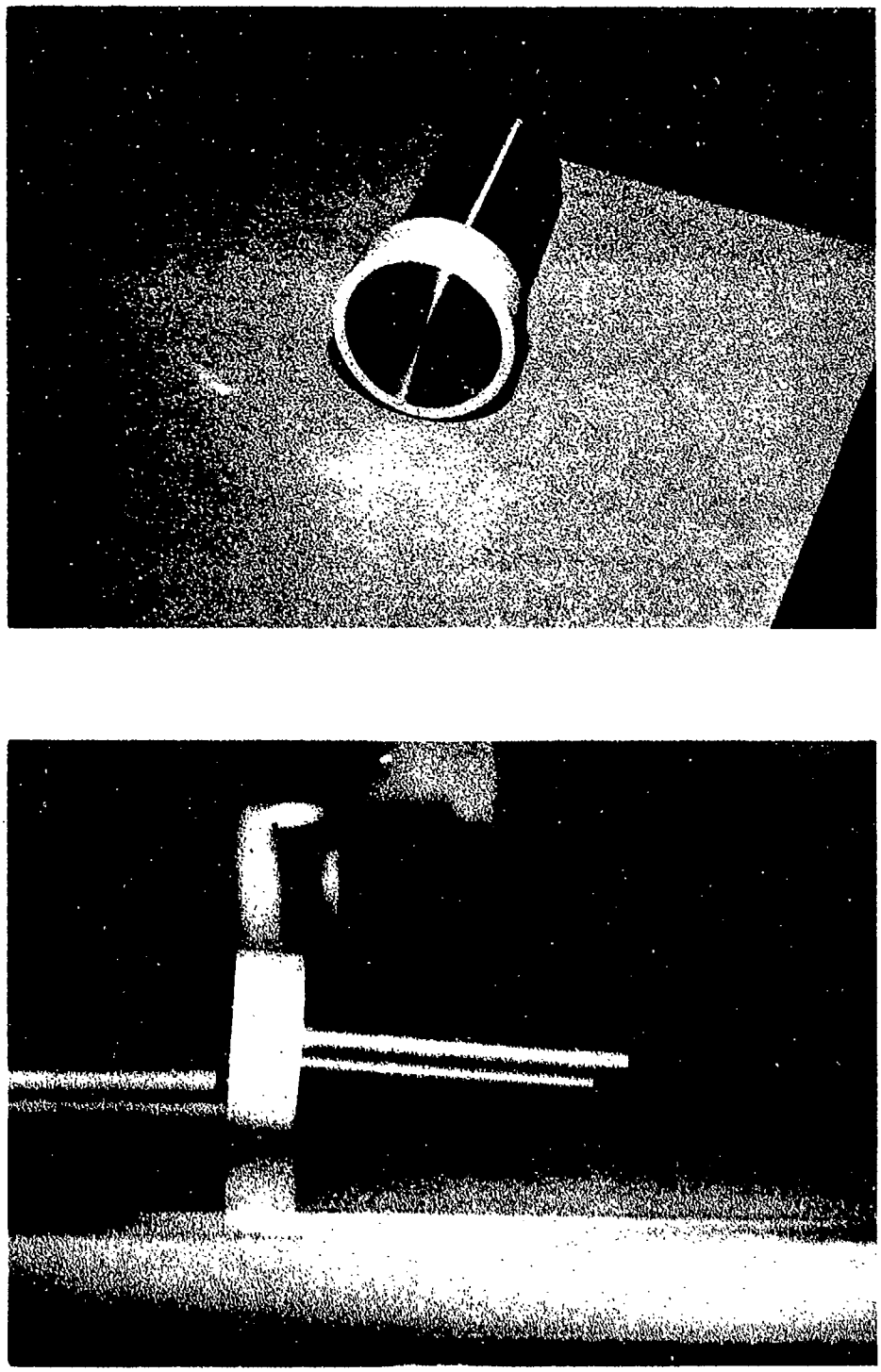

FIGURE 13. Photos of New Fixture Central Core

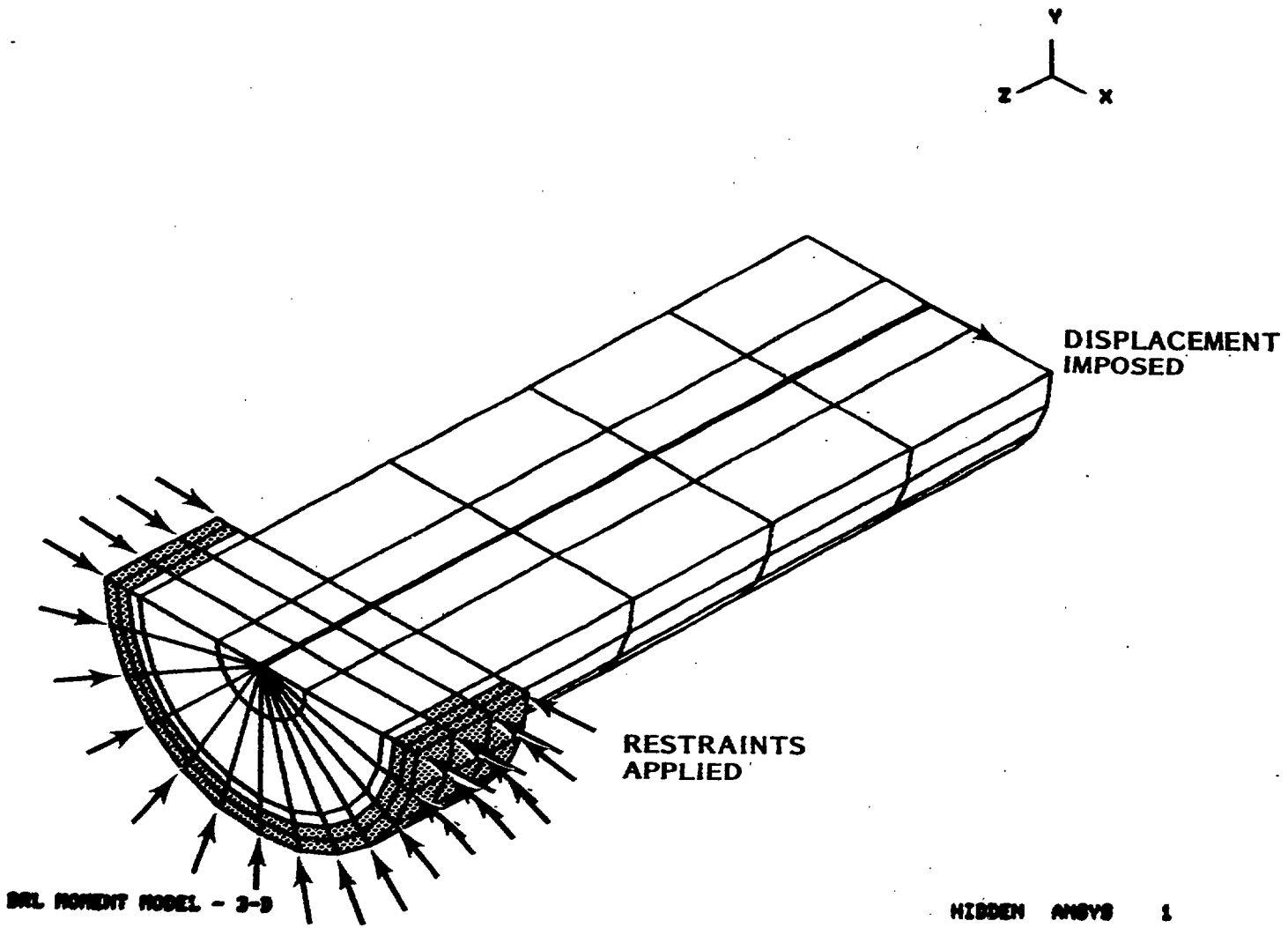

FIGURE 14. Finite Element Model of New Fixture Central Core

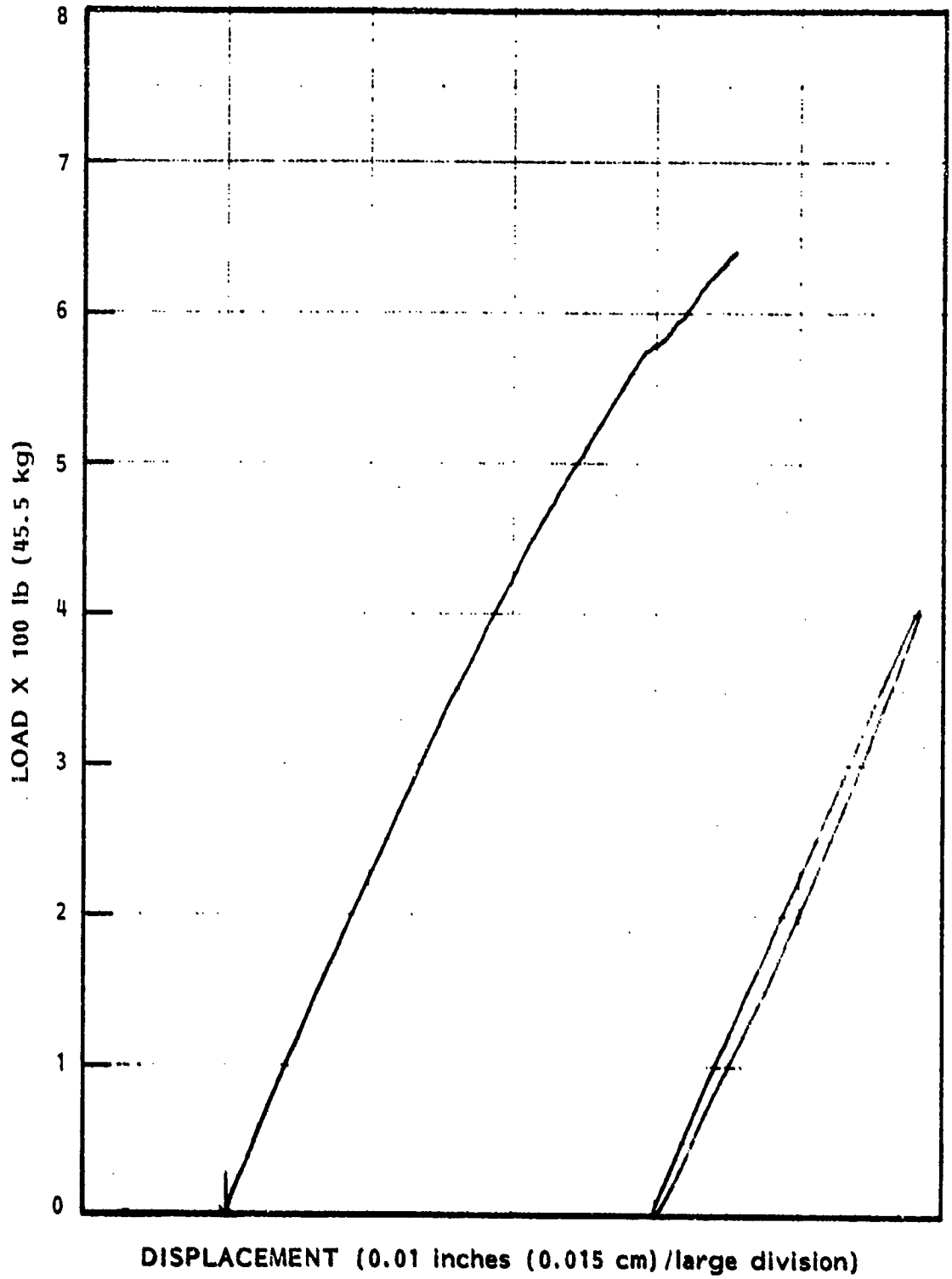

FIGURE 15. Test Results With New Central Core Portion

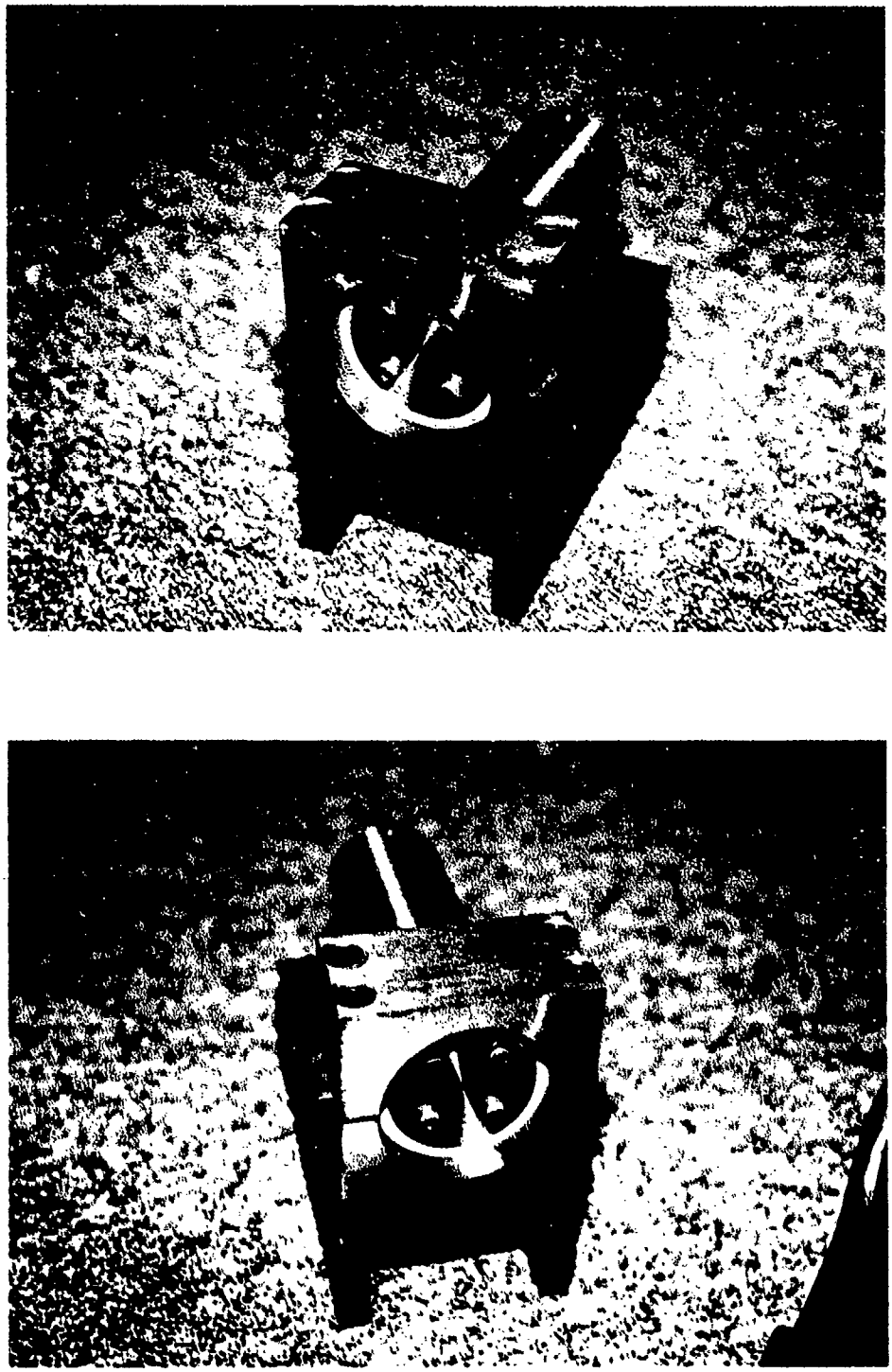

FIGURE 16. Photos of Newly Stiffened Fixture Assembled With Stainless Steel Central Core

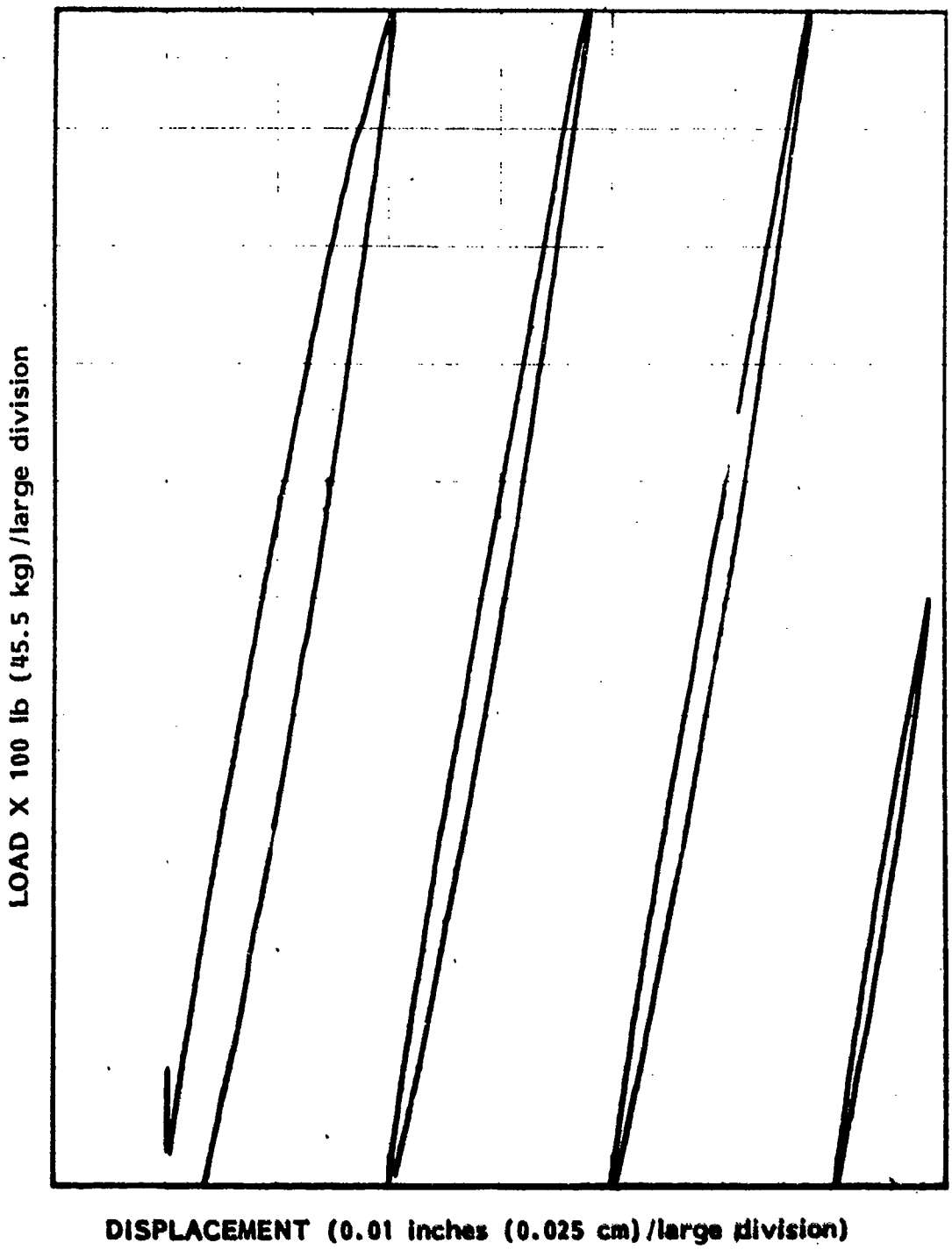

FIGURE 17. Test Results With Newly Stiffened Fixture

BOUNDARY CONDITIONS - FIXED VERSUS SLIDING

The boundary conditions at the plastic-to-gun-bore interface are a critical aspect of the analysis. In order to model this interface using ANSYS, the outer nodes of the plastic band were assigned zero displacement values in specified directions. This essentially models the gun bore as a rigid boundary. These nodes could be fixed in the radial, axial or circumferential directions. The method used to generate the nodal points used a cylindrical coordinate system. In the convention of the ANSYS code this means that fixing a node in the X-direction was the same as fixing it in the radial direction. The Y-coordinate coresponded to the tangential (or θ) direction, and the Z-coordinate corresponded to the axial direction. Since the simulation did not include twisting of the projectile in-bore (i.e., a smooth bore bullet), the displacement in the θ-direction was not constrained. This leaves two options, nodes fixed only in the R-direction (radially), or in both the r and z directions (radial and axial). The test fixture had circumferential grooves machined into it as mentioned before, so it would seem reasonable to expect that the plastic would not slip axially in the test. In a gun tube, however, the plastic is always sliding axially along the bore surface. In this light, it is more reasonable to fix these points in the radial direction only when modeling actual projectile behavior. In order to both model the condition of the test fixture, and shed some light upon the actual foundation moment under launch conditions, both of these cases were analyzed. The analyses of these two cases produced some surprising results. If we assume that the end deflection of the bar is 0.1 in. (0.25 cm) as before, ANSYS predicted reaction forces of 1314 lbf (597 kg) when only radial displacements were fixed and 7280 lbf (3305 kg) for the case where the outer plastic nodes were fixed in both the radial and axial directions. This is a factor of over 5.5 difference between the two cases.

A closed-form calculation was performed in an attempt to explain this large difference in predicted load. The idea behind this calculation is to evaluate the ratio of moment with frictionless sliding at the bore contact surface to moment with no sliding at this interface. Essentially, the shear stiffness of the plastic band contributes to the moment in the no-sliding case. The results of this computation are given below in Table 1. The details of the analysis are provided in an appendix of this report, as are definitions of the terms in the equations.

TABLE 1. LOAD RATIO FROM ANSYS AND COMPUTATION

$$\text{Load Ratio} = \frac{\text{Load with Frictionless Sliding}}{\text{Load with No Sliding}}$$

$$\text{ANSYS Runs:} \quad \text{Load Ratio} = \frac{1314 \text{ lbf } (597 \text{ kg})}{7280 \text{ lbf } (3305 \text{ kg})} \approx 0.18$$

$$\text{Closed-Form Estimate:} \quad \text{Load Ratio} = \frac{1}{1 + 6 \dfrac{R\,(R - t)}{\ell^2\,(1 + \nu)}} \approx 0.16$$

This estimation shows that a very large difference is expected for the two alternative boundary conditions. Several assumptions were made in the closed-form estimate, and these contribute to the difference with the ANSYS solution. The assumptions are also detailed in the appendix of this report which describes the closed-form analysis.

As was noted in the previous section of this report, the data from the test lie somewhere between the two cases. Table 2 is a listing of the results of a sensitivity study performed upon changing both the elastic modulus of the plastic band and the type of imposed boundary conditions. All of the predicted forces in Table 2 are for a 0.02 in. (0.05 cm) imposed deflection at the moment applying end of the ANSYS model.

TABLE 2. ANALYSIS RESULTS VARYING E_{NYLON} AND BOUNDARY CONDITIONS

E_{Nylon} (psi)	E_{Nylon} (MPa)	Fixity	Force Predicted by ANSYS (lbf)	Force Predicted by ANSYS (kg)
175,000	(1207)	Radial	268	(122)
175,000	(1207)	Radial + Axial	1,456	(661)
370,000	(2550)	Radial	540	(245)
370,000	(2550)	Radial + Axial	2,683	(1218)
600,000	(4130)	Radial	829	(376)
600,000	(4130)	Radial + Axial	3,780	(1716)

Two trends are immediately apparent upon examining this table. First, the boundary conditions imposed upon the model are very important in determining the predicted system stiffness. In all cases there is at least a factor of 4.5 difference in predicted force between the two alternate boundary conditions. Second, the relationship between the elastic modulus of the band and foundation moment is not linear. An increase in elastic modulus by a factor of two does not increase the stiffness of the system by a factor of two. This is at least partly because deformation of the steel core plays an increasing role in the flexing of the fixture with increasing band stiffness. This result shows that modelling the metallic parts as rigid is not a valid assumption. It also shows that the interaction between obturator and sabot, and the deformations of the metallic parts of any projectile play a significant role in determining the magnitude of the system stiffness and contribute to the balloting response of the projectile. Any design strategy which deals with foundation moment must therefore include the compliance of the metallic parts of the projectile.

MATERIAL PROPERTIES TESTS

The only mechanical properties available for the specific plastic used to fabricate the band were minimum manufacturer's specifications. As such, it was decided that material characterization tests for the plastic were necessary to permit detailed comparisons of finite element predictions with test results. Both the low strain rate and moderately high strain rate regions were of interest since the elastic modulus and yield strength of the plastic were believed to change with changing strain rate. Both properties were expected to increase with strain rate.

Initial mechanical properties tests were performed using some extruded ZYTEL 101 bar stock that was available in PNL's Materials Department from another project. Figure 18 shows the tensile specimens machined from this material. Initially, those specimens were machined from this bar stock. All three were machined from longitudinal sections of the bar; i.e., the long axis of the specimens was in the extrusion direction of the bar. The first specimen was pulled in tension to failure in an Instron tensile test machine. This was the "low strain rate" test. The head speed (rate of elongation of the specimen) was .02 in./min (0.051 cm/min). Another low strain rate test was performed in a similar manner except that the material was stressed above yield, then unloaded, and then cycled up to a stress above yield again. This cycling was repeated four times, and then the specimen was pulled in tension to failure. This cyclic testing was performed to study the anelastic or hysteresis behavior of the nylon material. The test results do show a significant amount of this type of behavior. This behavior was studied in this fashion because of the hysteresis seen in the bench tests (Figures 15 and 17). The shape of the Instron test curve is in fact very similar to that seen in the bench tests.

The third specimen was pulled to failure in tension at a high rate of strain. The specimen was loaded into a drop tower and impacted by a falling

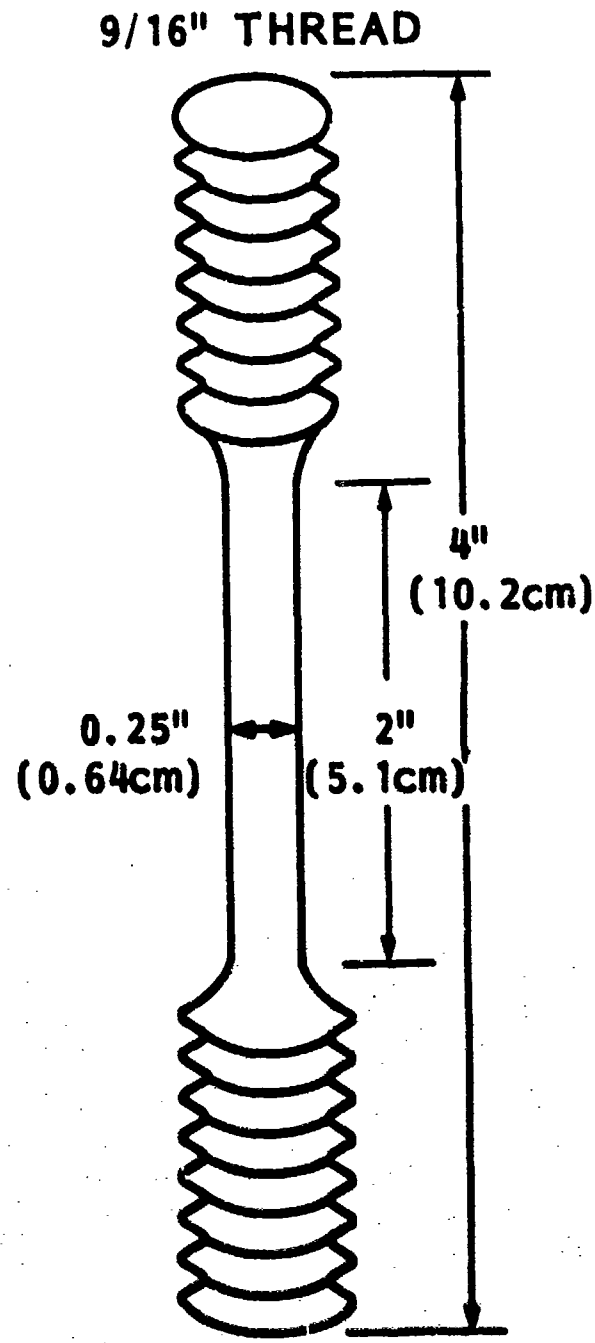

FIGURE 18. Cross Section View of Zytel 101 Tensile Test Specimens

weight. The velocity of the falling weight was 3180 in./min (8077 cm/min). This yields strain rates 160,000 times higher than those used in the slow rate tests. The entire high strain rate testing event took place in 3.12 msec from the initial impact. Results from the high strain rate (dynamic) and low strain rate (static) tests are summarized in Figure 19. The elastic modulus for the low rate of strain tests is 370,000 psi (2250 MPa) and for the high rate of strain tests it is 520,000 psi (3590 MPa) for this particular nylon. The third sample, before impact testing, was also tested ultrasonically to determine the dynamic modulus of elasticity. This test produced a modulus of 520,000 psi (3590 MPa), as in the impact test.

Test specimens were also cut from the centrifugally cast tube bought for this project. These specimens were cut from the same material as the nylon bands used in the bench test fixture. Three tensile specimens, identical to those used previously, and one compression specimen (a cylinder 2-1/2 in. (6.4 cm) long and 3/4 in. (1.9 cm) in diameter) were cut from this material. One of the tensile specimens was placed in a bucket of water overnight before testing to determine the effect of water absorption on the mechanical properties of the nylon material. Two of the tensile specimens were tested statically (low strain rate): one dry (65% relative humidity in the lab at the time) and one wet (out of the bucket of water). These two were tested ultrasonically before being pulled to failure on the Instron. The third tensile specimen cut from the tube was loaded into the drop tower and tested dynamically (high strain rate). The compression specimen was tested in the Instron at the low strain rate.

A summary of the results of all of the nylon mechanical properties tests performed for this project is provided in Table 3. There are a few important things to note in this table. First, the elastic modulus of the delivered nylon product is considerably above minimum manufacturers' specifications. These specifications were taken directly from the

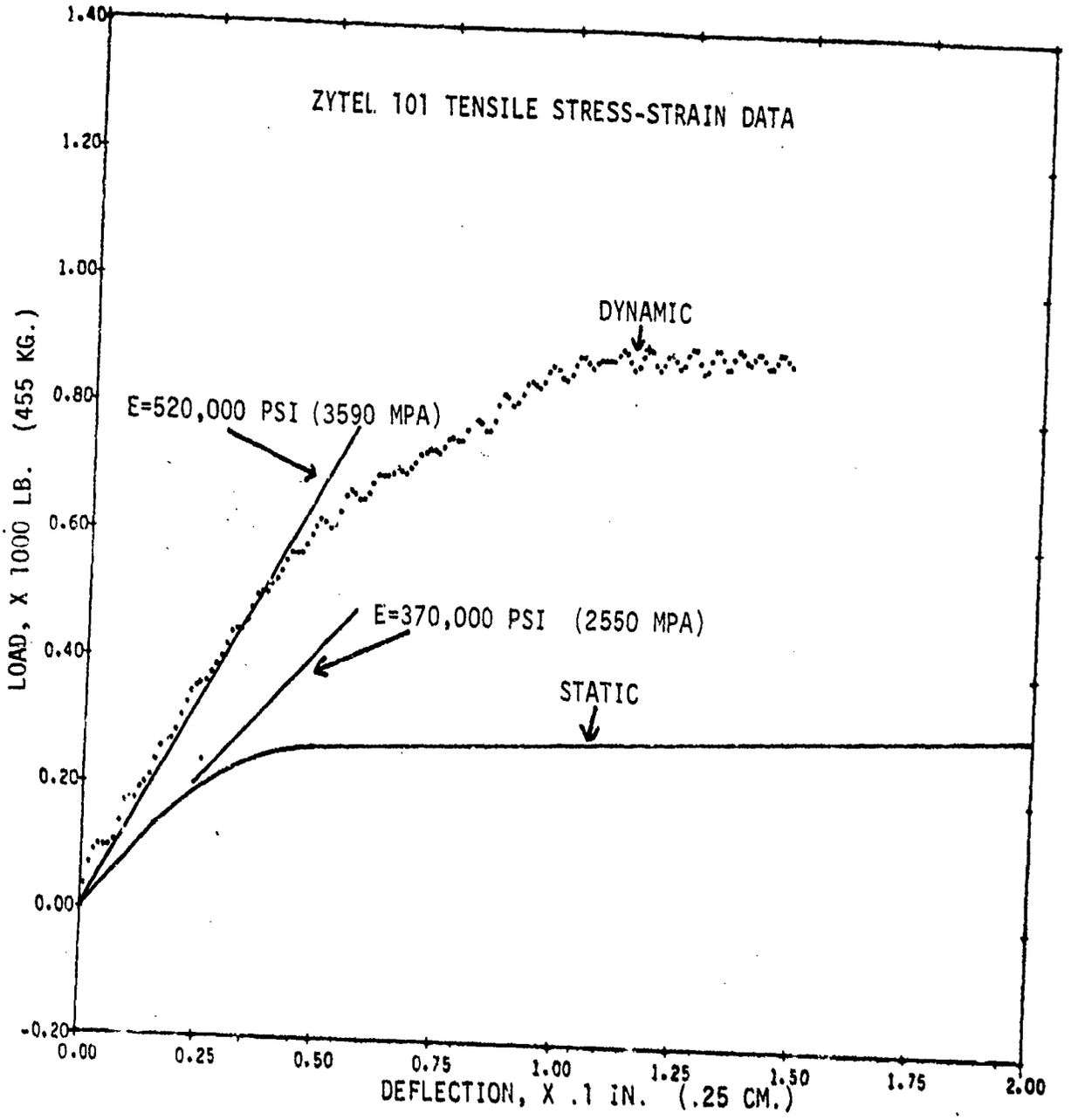

FIGURE 19. Summary of Dynamic and Static Tests Performed on Zytel 101 Extruded Bar Specimens

TABLE 3. SUMMARY OF MECHANICAL PROPERTIES TESTS

Mode	Material	Condition	Young's Modulus		Yield Strength (.2%)		Ultimate Strength	
			x 10^3 psi	MPa	x 10^3 psi	MPa	x 10^3 psi	MPa
Tension								
Low Strain Rate	Extruded Bar	Dry*	370	2550	7.4	51	13.0	90
	C. Cast	Dry	495	3410	7.3	51	11.4	79
	C. Cast	Wet**	474	3270	7.2	50	10.8	74
High Strain Rate	Extruded Rod	Dry	526	3630	11.6	80	18.4	128
	C. Cast	Dry	600	4140	10.9	75	16.2	112
Compression								
Low Strain Rate	C. Cast	Dry	605	4170	--	--	--	---
Ultrasonic	Extruded Rod	Dry	520	3590	--	--	--	---
	C. Cast	Dry	610	4210	--	--	--	---
	C. Cast	Wet	612	4220	--	--	--	---

* Dry = 65% Relative Humidity.
**Wet = sat in a bucket of water overnight.

manufacturers' specifications. Another handbook of material properties of plastics [2] quotes a somewhat higher modulus for the product. This reference quotes 350,000 psi (2410 MPa) for cast nylon type 6 and 200,000 psi (1380 MPa) for nucleated nylon type 66. The variability in quoted mechanical properties points to a second important conclusion to be drawn from the mechanical properties tests. That is that even Young's modulus is different for different product forms and possibly even for different lots of the same material. This is not the case in metals. Thus, it is not reasonable to treat these plastics in our simulation as we would metals.

Another rather important note to be made relates to the effects of rate of strain upon the mechanical properties of nylon. Within the same lot of material, the rate at which the material is strained determines in part the elastic response of the material. Both of the materials tested (extruded bar and spin-cast tube) exhibit this behavior. The rate of strain imposed upon the impact test specimens was similar to what could be expected to occur during launch of a projectile.

[2] *Modern Plastics Encyclopedia, October 1975, Volume 52, Number 10A, McGraw-Hill Publications Company, New York, NY.*

IMPLICATIONS OF RESULTS

Historically, it has been assumed that the foundation moment for a single bore contact projectile is rather small and would have a second order effect on projectile motion. The results of this project indicate that the foundation moment in a short wheel base round is not a neglectable effect. This will be shown with a relatively simple calculation.

If we presume

- that the modulus is more likely to be near 600,000 psi (431 MPa) as a consequence of the materials test,
- that the lower values for the moment are more nearly correct (the sliding case), and
- that the results are amenable to linear scaling,

then the calculations can be made to evaluate the effective magnitude of the restoring moment for a 120-mm projectile (KE). For a deflection of 0.02 in. (0.051 cm) related to the test apparatus, the net foundation moment generated for the 2.8 in. (70 mm) diameter band can be computed from

$$M_{70} = F\ d$$
$$= (829\ \text{lbf})^{*}\ (5.5\ \text{in.})$$
$$= 4565\ \text{in.-lbf}\ (5264\ \text{cm-Kg})$$

Now estimating the moment for a 120-mm diameter projectile, presuming that the length and thickness of the band are unchanged, gives

$$M_{120} = M_{70}\left(\frac{120}{70}\right)$$
$$= (4565\ \text{in.-lbf})\left(\frac{120}{70}\right)$$
$$= 7825\ \text{in.-lbf}$$
$$M_{120} \approx 7800\ \text{in.-lbf}\ (8995\ \text{cm-Kg})$$

*This value is taken directly from Table 2 for a nylon Young's modulus of 600,000 psi (4137 MPa) and fixed R-direction only.

The 0.02 in. (0.051 cm) deflection at the moment applying end is equivalent to about 0.21 degrees of angular deflection. To calculate the value of the peak moment generated by having the center of mass of the projectile at some axial distance from the position of the obturator band (the hinge) and at the same angle, we will assume a peak axial acceleration of 50,000 g's and a projectile weight of 16 lbm (7.26 Kg).* The resulting moment is given by

$$M_{acc} = (F_{acc})\ (\tan \alpha)\ (\ell)\ ,$$

where

M_{acc} = peak moment due to acceleration.

F_{acc} = body force due to acceleration = mass of round x axial acceleration (16 lbm) x (50,000 g's) = 800,000 lbf (363,200 Kg)

α = angular displacement, and

ℓ = axial distance between center of gravity and center of obturator band.

We can now solve for ℓ_{min} by equating the two moments, or

$$\ell_{min} = \frac{M_{acc}}{F_{acc} \tan \alpha}$$

$$= \frac{7800 \text{ in.-lbf}}{(800{,}000 \text{ lbf})\ (\tan .21^{0})}$$

$$= 2.68 \text{ in. } (6.81 \text{ cm})$$

In other words, the foundation moment in this case will equal the peak torque produced by the center of gravity being about 0.6 caliber ahead of the axial center of the obturator band. If the band restoring moment turns out to be greater, or if times other than peak propelling gas pressure are considered, the foundation moment is even more important.

*These figures are representative of a 120-mm KE bullet.

It should be recalled that several assumptions were made in the above calculation. For example, instead of using the results of the bench tests in which sliding was restrained, we used the results of the analysis of the same geometry in which sliding was permitted. The properties of the plastic were taken from results of mechanical properties tests. Linearly elastic behavior with no yielding was assumed. The measured yield strength of the plastic is about 12 kpsi (82.7 MPa), and the outer portion of the plastic in the analysis showed a stress of approximately that magnitude. Also, the analysis results were scaled from a 2.8 in. (70 mm) assembly to a 4.7 in. (120 mm) assembly.

If any one of the above assumptions is invalid, the comparison calculation could be inaccurate. We believe, however, that the assumptions made yield results that are conservative in the event that they are inaccurate. It, therefore, seems reasonable to expect that the foundation moment is a large effect and must be included in any calculation involving the dynamics of an in-bore projectile. There are several parameters to the problem which, however, warrant further investigation. Bench tests should be performed with a model projectile sliding within a model gun tube. Different grades of plastics should be used: for example, centrifugally cast versus extruded material. This will show the effect of typical variations in the mechanical properties of the plastic band material. The geometry of the band should also be changed to assess the effects of changing the thickness of the band and the length of the bore contact surface. Finally, the importance of the hysteresis must be explored as a damping mechanism for balloting motion.

REFERENCES

1. DuPont Plastics Design Handbook, page 15, Table 5.

2. Modern Plastics Encyclopedia, October 1975, Volume 52, Number 10A, McGraw-Hill Publications Company, New York, NY.

APPENDIX A

CLOSED-FORM ESTIMATION OF APPARENT DISCREPANCY IN THE TWO BOUNDARY CONDITION CASES

APPENDIX A

This appendix contains a calculation to resolve the apparent discrepancy in analysis results for the two different boundary condition cases: sliding or no sliding. In the sliding case, the gun bore-nylon interface is modeled as friction free and only the radial compliance of the nylon withstands the applied moment. In the no-sliding case, both the radial compliance and the shear stress at the gun bore-nylon interface will withstand the moment.

Figure A-1 portrays symbolically the two different boundary condition cases. The upper portion shows the sliding friction free case, and the lower portion shows the no-sliding case. Let us define terms as follows:

ℓ = length of gun bore to nylon interface (width of obturator)

t = thickness of nylon

R = radius of center of projectile

r = radial position or direction

z = longitudinal or down-bore direction

E = nylon Young's modulus

G = nylon shear modulus = $\frac{E}{2(1+\nu)}$

ν = nylon Poisson's Ratio

θ = rotation of projectile about the center - this rotation causes the moment

u = displacement in the radial direction (r direction)

v = displacement in the longitudinal direction (z direction).

First, we will look at the no-sliding case. The relationship between shear stress and shear strain can be given by Hooke's Law as follows:

$$\tau = G\left(\frac{du}{dz} + \frac{dv}{dr}\right)$$

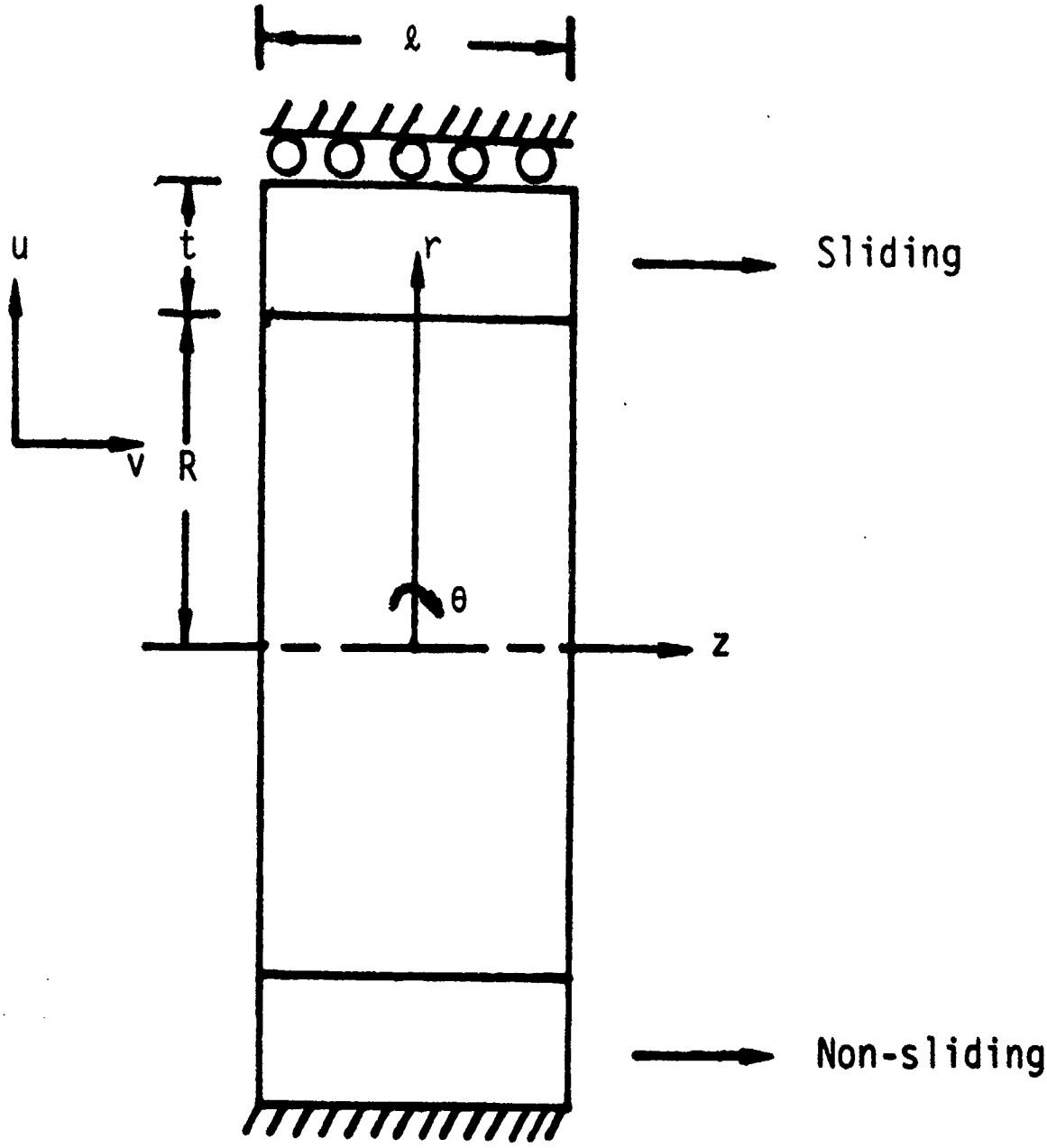

FIGURE A-1. Idealization of Test Fixture Geometry Showing Both Boundary Condition Cases: Sliding (Top) and Nonsliding (Bottom)

Our displacement relationships are as follows:

$$\text{at } r = R \quad , \quad v \simeq R\theta$$

$$\text{at } r = R + t \quad , \quad v = 0$$

and in general

$$v = - R\theta \left(\frac{r - R - t}{t}\right)$$

For sliding and no sliding, the u-displacements are as follows

$$u \simeq - v \, (z/R)$$

$$\simeq - R\theta \, (z/R) \left[\frac{r - R - t}{t}\right]$$

or

$$u \simeq - z\theta \left[\frac{r - R - t}{t}\right]$$

Now, going back to our shear stress/strain relationships

$$\tau = G \left[\frac{du}{dz} + \frac{dv}{dr}\right]$$

and differentiating

$$\tau = G \left[- \theta \left(\frac{r - R - t}{t}\right) - \frac{R\theta}{t}\right]$$

$$\tau = - \frac{G\theta}{t} \, [r - R - t + R] = - \frac{G\theta}{t} \, [r - t]$$

and for $r = R$

$$\tau = \frac{G\theta}{t} \, [R - t]$$

and the moment due to this shear stress can be given by

$$M_{shear} = 2 \, \tau \, \ell \, R$$

$$= \frac{2 \, G\theta \, \ell \, R \, (R - t)}{t}$$

and from our shear modulus/Young's modulus relationships

$$M_{shear} \propto \frac{E\,\theta\,\ell\,R\,(R - t)}{t\,(1 + \nu)}$$

The radial stress at any point, σ_r, can be given by

$$\sigma_r \propto E\,\frac{du}{dr} = E\,[-\theta z\,(1/t)]$$

$$\sigma_r \propto -\frac{E\,\theta\,z}{t}$$

and the moment due to this radial stress can be given by

$$M_{radial} = 2\int_{-\ell/2}^{\ell/2} z\,\sigma_r\,dz$$

$$= -2\,\frac{E\theta}{t}\int_{-\ell/2}^{\ell/2} z^2\,dz$$

$$= -2\,\frac{E\theta}{t}\left[\frac{z^3}{3}\right]_{-\ell/2}^{\ell/2}$$

$$= \frac{-E\theta\ell^3}{6t}$$

Now, what we want is a measure of the difference between the two boundary condition cases, or a ratio as follows

$$\text{Ratio} = \frac{\text{Moment due to } \sigma_r}{\text{Moment due both to } \sigma_r \text{ and } \tau}$$

or

$$\text{Ratio} = \frac{E\theta\ell^3/6t}{E\theta\ell^3/6t + \frac{E\theta\ell R\,(R - t)}{t\,(1 + \nu)}}$$

or, after some algebraic manipulation

$$\text{Ratio} = \frac{1}{1 + 6 \dfrac{R\,(R - t)}{\ell^2\,(1 + \nu)}}$$

Taking values of the dimensions from our test fixture, as follows:

$t = 0.2$ in. (0.51 cm)
$R = 1.2$ in. (3.05 cm)
$\ell = 1.0$ in. (2.54 cm)
$\nu = 0.386$ (from material test data)

Then the ratio can be evaluated as follows

$$\text{Ratio} = \frac{1}{1 + 6 \dfrac{(1.2)\,(1.2 - .2)}{(1.0)^2\,(1 + .386)}}$$

$$\text{Ratio} = 0.16$$

From our finite element results, the ratio of results can be evaluated as follows and compared to the closed-form solution:

$$\text{Ratio From Finite Element Results} = \frac{1314}{7280}$$

$$\text{Ratio Calculated} = 0.18$$

The closed-form estimate is based upon many assumptions, such as a rigid representation of the metal parts. The difference between the 0.16 calculated closed form and the 0.18 calculated using ANSYS is therefore not considered significant. The fact that the ratio is so small, or that the shear stress plays such a major role in determining the moment is, however, a significant finding.

DISTRIBUTION LIST

No. of Copies	Organization
12	Administrator Defense Technical Info Center ATTN: DTIC-DDA Cameron Station Alexandria, VA 22314
1	Director of Defense Research & Engineering (OSD) ATTN: Mr. R. Thorkildsen Washington, DC 20301
1	Director of Defense Research & Engineering (OSD) ATTN: Mr. J. Persh Washington, DC 20301
1	Director Defense Advanced Research Projects Agency 1400 Wilson Boulevard Arlington, VA 22209
1	Director Institute of Defense Analysis ATTN: Documents Acquisition 1801 Beauregard St. Alexandria, VA 22311
1	HQDA (DAMA-MS) Washington, DC 20310
1	HQDA (DAMA-ZA) Washington, DC 20310
1	HQDA (DAMA-ZD, H. Woodall) Washington, DC 20310
1	HQDA (DAMA-ARZ-A, Dr. M.E. Lasser) Washington, DC 20310
2	HQDA (DAMA-CSM-VA) (DAMA-CSM-CA) Washington, DC 20310
1	HQDA (DAMA-CSS-T, Dr. J. Bryant) Washington, DC 20310
1	Commander US Army Materiel Development and Readiness Command ATTN: DRCDMD-ST 5001 Eisenhower Avenue Alexandria, VA 22333
1	Commander US Army Materiel Development and Readiness Command ATTN: DRCLDC, Mr. T. Shirata 5001 Eisenhower Avenue Alexandria, VA 22333
1	Commander US Army Materiel Development and Readiness Command ATTN: DRCDE, Dr. R.H. Haley Deputy Director 5001 Eisenhower Avenue Alexandria, VA 22333
1	Commander US Army Materiel Development and Readiness Command ATTN: DRCDE-R 5001 Eisenhower Avenue Alexandria, VA 22333
1	Commander US Army Materiel Development and Readiness Command ATTN: Mr. Lindwarm 5001 Eisenhower Avenue Alexandria, VA 22333
8	Commander USA ARRADCOM ATTN: DRDAR-LCA, Mr. A. Moss DRDAR-LC, J.T. Frasier DRDAR-SE DRDAR-SA DRDAR-AC DRDAR-LCU-SE, E. Pearson DRDAR-LCA-M, F. Saxe DRDAR-LCU-SS, R. Botticelli Dover, NJ 07801

DISTRIBUTION LIST

No. of Copies	Organization
5	Commander USA ARRADCOM ATTN: DRDAR-SCS, Mr. D. Brandt DRDAR-SCS-E, Mr. J. Blumer DRDAR-SCF, Mr. G. Del Coco DRDAR-SCS, Mr. S. Jacobson DRDAR-SCF, Mr. K. Pfleger Dover, NJ 97801
2	Commander USA ARRADCOM ATTN: DRDAR-TSS Dover, NJ 07801
4	Commander USA ARRADCOM ATTN: DRDAR-TD DRDAR-TDA DRDAR-TDS DRDAR-TDC, Dr. D. Gyorog Dover, NJ 07801
5	Commander USA ARRADCOM ATTN: DRDAR-LCU, Mr. E. Barrieres DRDAR-LCU, Mr. R. Davitt DRDAR-LCU-M, Mr. D. Robertson DRDAR-LCU-M, Mr. M. Weinstock DRDAR-LCA-M, Mr. C. Larson Dover, NJ 07801
7	Commander USA ARRADCOM ATTN: DRDAR-LCA, Mr. B. Knutelski DRDAR-LCR-R, Mr. E.H. Moore III DRDAR-LCS, Mr. J. Gregorits DRDAR-LCS-D, Mr. K. Rubin DRDAR-LCA, Dr. T. Davidson DRDAR-LCA, E. Friedman DRDAR-LCA, A. Lehberger Dover, NJ 07801
7	Commander USA ARRADCOM ATTN: DRDAR-SCA, C.J. McGee DRDAR-SCA, S. Goldstein DRDAR-SCA, F.P. Puzychki DRDAR-SCA, E. Jeeter DRDAR-SCF, M.J. Schmitz DRDAR-SCF, L. Berman DRDAR-SCZ, P. Petrella Dover, NJ 07801
9	Commander USA ARRADCOM ATTN: DRDAR-SCM DRDAR-SCM, Dr. E. Bloore DRDAR-SCM, Mr. J. Mulherin DRDAR-SCS, Mr. B. Brodman DRDAR-SCS, Dr. T. Hung DRDAR-SCA, Mr. W. Gadomski DRDAR-SCA, Mr. E. Malatesta DRDAR-SCA-T, P. Benzkofer DRDAR-SCA-T, F. Dahdouh Dover, NJ 07801
3	Commander USA ARRADCOM ATTN: DRDAR-LCA, Mr. W. Williver DRDAR-LCA, Mr. S. Bernstein DRDAR-LCA, Mr. G. Demitrack Dover, NJ 07801
4	Commander USA ARRADCOM ATTN: DRDAR-LCA, Dr. S. Yim DRDAR-LCA, Mr. L. Rosendorf DRDAR-LCA, Dr. S.H. Chu DRDAR-LCW, Mr. R. Wrenn Dover, NJ 07801
6	Director USA ARRADCOM Benet Weapons Laboratory ATTN: DRDAR-LCB-TL DRDAR-LCB, Mr. Rummel DRDAR-LCB-RA, Mr. R. Scanlon DRDAR-LCB-RM, Mr. M. Scarullo DRDAR-LCB-RA, Mr. R. Soanes, Jr. DRDAR-LCB-RA, Dr. J. Vasilakis Watervliet, NY 12189

DISTRIBUTION LIST

No. of Copies	Organization
7	Director USA ARRADCOM Benet Weapons Laboratory ATTN: DRDAR-LCB-RA, Dr. T. Simkins DRDAR-LCB-D, Dr. J. Zweig DRDAR-LCB-RA, Mr. G. Pflegl DRDAR-LCB-M, Mr. J. Purtell DRDAR-LCB-RA, Dr. R. Racicot DRDAR-LCB-DS, Dr. J. Santini DRDAR-LCB-RA, Dr. J. Wu Watervliet, NY 12189
2	Commander USA ARRADCOM ATTN: DRDAR-SC, Mr. B. Shulman DRDAR-SC, Mr. Webster Dover, NJ 07801
1	Commander USA ARRADCOM ATTN: DRDAR-SE Dover, NJ 07801
2	Commander USA ARRADCOM ATTN: Army Fuze Mgt Project Office DRDAR-FU Dover, NJ 07801
2	Commander USA ARRADCOM ATTN: Development Project Office for Selected Ammunitions DRDAR-DP Dover, NJ 07801
2	Commander USA ARRADCOM ATTN: Product Assurance Directorate DRDAR-QA Dover, NJ 07801
1	Commander USA ARRADCOM ATTN: DRDAR-NS Dover, NJ 07801
1	Commander USA ARRADCOM ATTN: L. Goldsmith Dover, NJ 07801
1	Commander US Army Rock Island Arsenal ATTN: DRDAR-TSE-SW, R. Radkiewicz Rock Island, IL 61299
2	Commander US Army Armament Materiel Readiness Command ATTN: DRDAR-LEP-L DRDAR-TSE-SW, G. Strahl Rock Island, IL 61299
1	Commander US Army Armament Materiel Readiness Command ATTN: SARRI-RLS, Mr. J.B. Ackley Rock Island, IL 61299
1	Commander US Army Aviation Research and Development Command ATTN: DRDAV-E 4300 Goodfellow Blvd. St. Louis, MO 63120
1	Director US Army Air Mobility Research and Development Laboratory Ames Research Center Moffett Field, CA 94035
2	Director US Army Air Mobility Research and Development Laboratory ATTN: Dr. Hans Mark Dr. R.L. Cohen Ames Research Center Moffett Field, CA 94035
2	Director US Army Research and Technology Laboratories (AVRADCOM) Ames Research Center Moffett Field, CA 94035

DISTRIBUTION LIST

No. of Copies	Organization
3	Director US Army Research and Technology Laboratories ATTN: DAVDL-AS, Mr. W. Andre(2 cys), DAVDL-AS, Dr. R.M. Carlson Ames Research Center Moffett Field, CA 94035
1	Commander US Army Communications Research and Development Command ATTN: DRSEL-ATDD Fort Monmouth, NJ 07703
1	Commander US Army Electronics Research and Development Command Technical Support Activity ATTN: DELSD-L Fort Monmouth, NJ 07703
1	Commander Atmospheric Sciences Laboratory US Army Electronics Research and Development Command ATTN: DELAS-EO-MO, Dr. R.B.Gomez White Sands Missile Range NM 88002
3	Commander US Army Harry Diamond Laboratories ATTN: DELHD-I-TR, H.D. Curchak DELHD-I-TR, H. Davis DELHD-S-QE-ES, Ben Banner 2800 Powder Mill Road Adelphi, MD 20783
1	Commander US Army Harry Diamond Laboratories ATTN: DELHD-TA-L 2800 Powder Mill Road Adelphi, MD 20783
1	Director Night Vision Laboratory Fort Belvoir, VA 22060
1	Commander US Army Missile Command ATTN: DRSMI-R Redstone Arsenal, AL 35898
2	Commandant US Army Infantry School ATTN: ATSH-CD-CSO-OR Fort Benning, GA 31905
1	Commander US Army Missile Command ATTN: DRSMI-YDL Redstone Arsenal, AL 35898
2	Commander US Army Missile Command ATTN: DRCPM-TO DRCPM-HD Redstone Arsenal, AL 35898
1	Commander US Army Mobility Equipment Research & Development Command Fort Belvoir, VA 22060
2	Commander US Army Tank Automotive Command ATTN: DRSTA-TSL DRSTA-ZSA, Dr. R. Beck Warren, MI 48090
1	Commander US Army Natick Research and Development Command ATTN: DRDNA-DT, Dr. Sieling Natick, MA 01762

DISTRIBUTION LIST

No. of Copies	Organization
1	Commander US Army Tank Automotive Command ATTN: DRSTA-NS Warren MI 48090
1	Director US Army TRADOC Systems Analysis Activity ATTN: ATAA-SL White Sands Missile Range, NM 88002
2	President US Army Armor and Engineering Board ATTN: ATZK-AE-CV ATZK-AE-IN, Mr. L. Smith Fort Knox, KY 40121
2	Commander US Army Research Office ATTN: Dr. R. Weigle Dr. E. Saibel P.O. Box 12211 Research Triangle Park NC 27709
3	Commander US Army Research Office P.O. Box 12211 ATTN: Technical Director Engineering Division Metallurgy & Materials Division Research Triangle Park, NC 27709
1	Commander US Army Research Office ATTN: Dr. J. Chandra Research Triangle Park, NC 27709
3	Project Manager Cannon Artillery Weapons System ATTN: DRCPM-CAWS Dover, NJ 07801
2	Project Manager Nuclear Munitions ATTN: DRCPM-NUC Dover, NJ 07801
2	Project Manager Tank Main Armament Systems ATTN: DRCPM-TMA Dover, NJ 07801
2	Project Manager Sergeant York ATTN: DRCPM-ADG Dover, NJ 07801
1	Product Manager for 30mm Ammo. ATTN: DRCPM-AAH-30mm Dover, NJ 07801
2	Product Manager M110E2 Weapon System, DARCOM ATTN: DRCPM-M110E2 Rock Island, IL 61299
4	Director US Army Materials and Mechanics Research Center ATTN: Director (3 cys) DRXMR-ATL (1 cy) Watertown, MA 02172
2	Commander US Army Materials and Mechanics Research Center ATTN: J. Mescall Tech. Library Watertown, MA 02172
1	Commander US Army Training and Doctrine Command ATTN: TRADOC Lib, Mrs. Thomas Fort Monroe, VA 23651
1	Commander US Army Armor School ATTN: Armor Agency, MG Brown Fort Knox, KY 40121

DISTRIBUTION LIST

No. of Copies	Organization
1	Commander US Army Field Artillery School ATTN: Field Artillery Agency Fort Sill, OK 73503
1	Commander US Army Infantry School ATTN: BG R.W. Riscassi Fort Benning, GA 31905
1	Superintendent Naval Postgraduate School ATTN: Dir of Lib Monterey, CA 93940
1	Commander US Army Combined Arms Combat Development Activity Fort Leavenworth, KS 66027
1	Commander US Army Combat Development Experimentation Command ATTN: Tech Info Center Bldg. 2925, Box 22 Fort Ord, CA 93941
1	Commander Naval Sea Systems Command ATTN: ORD-9132 Washington, DC 20362
1	Commander Naval Sea Systems Command (SEA-62R41) ATTN: L. Pasiuk Washington, DC 20362
1	Commander Naval Research Laboratory ATTN: Commander H. Peritt, Code R31 Washington, DC 20375
1	Commander David W. Taylor Naval Ship Research & Development Center Bethesda, MD 20084
4	Commander Naval Research Laboratory ATTN: Mr. W.J. Ferguson Dr. C. Sanday Dr. H. Pusey Dr. F. Rosenthal Washington, DC 20375
6	Commander Naval Surface Weapons Center ATTN: Code X211, Lib E. Zimet, R13 R.R. Bernecker, R13 J.W. Forbes, R13 S.J. Jacobs, R10 K. Kim, R13 Silver Spring, MD 20910
3	Commander Naval Surface Weapons Center ATTN: Code E-31, R.C. Reed M.T. Walchak Code V-14, W.M. Hinckley Silver Spring, MD 20910
5	Commander Naval Surface Weapons Center ATTN: Code G-33, T.N. Tschirn Code N-43, J.J. Yagla L. Anderson G. Soo Hoo Code TX, Dr. W.G. Soper Dahlgren, VA 22448

DISTRIBUTION LIST

No. of Copies	Organization
1	Commander Naval Weapons Center China Lake, CA 93555
1	Commander Naval Weapons Center ATTN: J. O'Malley China Lake, CA 93555
2	Commander Naval Weapons Center ATTN: Code 3835, R. Sewell Code 3431, Tech Lib China Lake, CA 93555
2	Commander US Naval Weapons Center ATTN: Code 608, Mr. R. Derr Code 4505, Mr. C. Thelen China Lake, CA 93555
3	Commander Naval Weapons Center ATTN: Code 4057 Code 3835 B. Lundstrom Code 3835 M. Backman China Lake, CA 93555
1	Commander Naval Ordnance Station Indian Head, MD 20640
2	Commander Naval Ordnance Station ATTN: Code 5034, Ch. Irish, Jr. T.C. Smith Indian Head, MD 20640
1	Office of Naval Research ATTN: Code ONR 439, N. Perrone Department of the Navy 800 North Quincy Street Arlington, VA 22217
1	Commandant US Marine Corps ATTN: AX Washington, DC 20380
2	AFATL Gun and Rocket Division ATTN: W. Dittrich; DLJM D. Davis; DLDL Eglin AFB, FL 32542
2	ADTC/DLJW Eglin AFB, FL 32542
1	ADTC/DLODL, Tech Lib Eglin AFB, FL 32542
1	AFWL/SUL Kirtland AFB, NM 87115
1	AFWL/SUL ATTN: J.L. Bratton Kirtland AFB, NM 87115
1	AFML (Dr. T. Nicholas) Wright- Patterson AFB, OH 45433
2	ASD (XROT, G. Bennett; ENFTV, Martin Lentz) Wright-Patterson AFB, OH 45433
1	New Mexico Institute of Mining and Technology Terra Group Socorro, NM 87801
2	Battelle Memorial Institute ATTN: Dr. L. E. Hulbert Mr. J. E. Backofen, Jr. 505 King Avenue Columbus, OH 43201

DISTRIBUTION LIST

No. of Copies	Organization
3	Battelle Pacific Northwest Laboratory ATTN: E.M. Patton Dr. F.A. Simonen L.A. Strope P.O. Box 999 Richland, WA 99352
1	Bell Telephone Laboratories, Inc. Mountain Avenue Murray Hill, NJ 07971
1	Director Lawrence Livermore Laboratory P.O. Box 808 Livermore, CA 94550
2	Director Lawrence Livermore Laboratory ATTN: E. Farley, L9 D. Burton, L200 Livermore, CA 94550
3	Director Lawrence Livermore Laboratory ATTN: Dr. R.H. Toland, L-424 Dr. M.L. Wilkins Dr. R. Werne Livermore, CA 94550
1	Director NASA - Ames Research Center Moffett Field CA 94035
2	Forrestal Research Center Aeronautical Engineering Laboratory ATTN: Dr. S. Lam Dr. A. Eringen Princeton, NJ 08540
1	Sandia National Laboratories ATTN: D.E. Waye Livermore, CA 94550
1	AFELM, The Rand Corporation ATTN: Library-D 1700 Main Street Santa Monica, CA 90406
1	Aircraft Armaments Inc. ATTN: John Hebert York Road & Industry Lane Cockeysville, MD 21030
2	ARES, Inc. ATTN: Duane Summers Phil Conners Port Clinton, OH 43452
2	AVCO Corporation Structures and Mechanics Department ATTN: Dr. W. Broding Mr. J. Gilmore Wilmington, MA 01887
3	BLM Applied Mechanics Consultants ATTN: Dr. A. Boresi Dr. R. Miller Dr. H. Langhaar 3310 Willett Drive Laramie, WY 82070
1	Martin Marietta Laboratories ATTN: Mr. J.I. Bacile Orlando, FL 32805
1	H. P. White Laboratory 3114 Scarboro Road Street, MD 21154
1	CALSPAN Corporation ATTN: E. Fisher P.O. Box 400 Buffalo, NY 14225
1	FMC Corporation Ordnance Engineering Division San Jose, CA 95114
1	Kaman-TEMPO ATTN: E. Bryant 715 Shamrock Road Bel Air, MD 21014

DISTRIBUTION LIST

No. of Copies	Organization
1	General Electric Company ATTN: Armament Systems Department D. A. Graham Lakeside Avenue Burlington, VT 05402
1	Olin Corporation Badger Army Ammunition Plant ATTN: R.J. Thiede Baraboo, WI 53913
1	S&D Dynamics, Inc. ATTN: Dr. M. Soifer 755 New York Avenue Huntington, NY 11743
1	Southwest Research Institute ATTN: P.A. Cox 8500 Culebra Road San Antonio, TX 78228
1	Southwest Research Institute ATTN: Mr. T. Jeter 8500 Culebra Road San Antonio, TX 78228
1	University of Dayton Research Institute ATTN: S.J. Bless Dayton, OH 45406
1	University of Delaware Department of Mechanical Engineering ATTN: Dr. H. Kingsbury Newark, DE 19711
1	University of Illinois Aeronautical and Astronautical Engineering Department 101 Transportation Building ATTN: Prof. Adam Zak Urbana, IL 61801
2	University of Iowa College of Engineering ATTN: Dr. R. Benedict Dr. E.J. Haug Iowa City, IA 52240
1	Rutgers University Dept. of Mechanical and Aerospace Engineering P.O. Box 909 ATTN: Dr. T.W. Lee Piscataway, NJ 08854
1	University of Wisconsin Mechanical Engineering Department ATTN: Prof. S.M. Wu Madison, WI 53706
1	University of Wisconsin Mathematics Research Center 610 Walnut Street ATTN: Prof. B. Noble Madison, WI 53706

Aberdeen Proving Ground

Dir, USAMSAA
ATTN: DRXSY-D
DRXSY-MP, H. Cohen
DRXSY-G, E. Christman
DRXSY-OSD, H. Burke
DRXSY-G, R.C. Conroy
DRXSY-LM, J.C.C. Fine
Dir, USAHEL
ATTN: DRXHE, A.H. Eckles, III
Cdr, USATECOM
ATTN: DRSTE-CE
DRSTE-TO-F
Dir, USACSL, Bldg. E3516, EA
ATTN: DRDAR-CLB-PA
DRDAR-CL
DRDAR-CLB
DRDAR-CLD
DRDAR-CLY
DRDAR-CLN
DRDAR-CLN-D, L. Shaff
DRDAR-CLN-D, F. Dagostin
DRDAR-CLN-D, C. Hughes
DRDAR-CLN, J. McKivrigan
DRDAR-CLJ-L

USER EVALUATION OF REPORT

Please take a few minutes to answer the questions below; tear out this sheet, fold as indicated, staple or tape closed, and place in the mail. Your comments will provide us with information for improving future reports.

1. BRL Report Number _____

2. Does this report satisfy a need? (Comment on purpose, related project, or other area of interest for which report will be used.)

_____

_____

_____

3. How, specifically, is the report being used? (Information source, design data or procedure, management procedure, source of ideas, etc.) _____

_____

_____

4. Has the information in this report led to any quantitative savings as far as man-hours/contract dollars saved, operating costs avoided, efficiencies achieved, etc.? If so, please elaborate.

_____

_____

5. General Comments (Indicate what you think should be changed to make this report and future reports of this type more responsive to your needs, more usable, improve readability, etc.) _____

_____

_____

_____

6. If you would like to be contacted by the personnel who prepared this report to raise specific questions or discuss the topic, please fill in the following information.

Name: _____

Telephone Number: _____

Organization Address: _____

_____

_____